

Landau Theory of Tilting of Oxygen Octahedra in Perovskites

A. B. Harris¹

¹*Department of Physics and Astronomy, University of Pennsylvania, Philadelphia PA 19104*

(Dated: November 7, 2018)

The list of possible commensurate phases obtained from the parent tetragonal phase of Ruddlesden-Popper systems, $A_{n+1}B_nC_{3n+1}$ for general n due to a single phase transition involving the reorienting of octahedra of C (oxygen) ions is reexamined using a Landau expansion. This expansion allows for the nonlinearity of the octahedral rotations and the rotation-strain coupling. It is found that most structures allowed by symmetry are inconsistent with the constraint of rigid octahedra which dictates the form of the quartic terms in the Landau free energy. For A_2BC_4 our analysis allows only 10 (see Table III) of the 41 structures listed by Hatch *et al.* which are allowed by general symmetry arguments. The symmetry of rotations for RP systems with $n > 2$ is clarified. Our list of possible structures in Table VII excludes many structures allowed in previous studies.

PACS numbers: 61.50.Ks, 61.66.-f, 63.20.-e, 76.50.+g

I. INTRODUCTION

The Ruddlesden-Popper (RP) compounds[1] are layered perovskites having the chemical formula $A_{n+1}B_nC_{3n+1}$ and which consist of two slabs of BC_6 octahedra per conventional unit cell. Each slab consists of n layers of corner sharing octahedra of F's or O's. These systems either are or can be considered to be developed via one or more structural transitions from the high symmetry tetragonal parent structure shown in Fig. 1 for the cases exemplified by K_2MgF_4 ($n = 1$) and $Ca_3Mn_2O_7$ ($n = 2$). We will refer to the RP system with $n = 1$ as RP214 and to that with $n = 2$ as RP327.

The RP systems exhibit many interesting technological

properties such as high T_c superconductivity[2], colossal magnetoresistance,[3] metal insulator transitions,[4] and coupled ferroelectric and magnetic order.[5–7] Many of these properties depend sensitively on the distortions from the ideal tetragonal $I4/mmm$ structure (see Fig. 1) of space group #139 [numbering of space groups is from Ref. 8] which appear at structural phase transitions.[9–13] Accordingly, the accurate characterization of their structure is essential to reach a detailed understanding of their properties. Such an understanding can potentially lead to the fabrication of new systems with enhanced desired properties. It is therefore not surprising that one of the most celebrated theoretical problems in crystallography is to list the possible structures that can result from a single structural phase transition in which the (usually oxygen) octahedra are cooperatively reoriented under the constraint that they are only distorted weakly (in a sense made precise below). One of the earliest works to address this question was that of Glazer[14] who analyzed possible structural distortion from the cubic parent structure of $CaTiO_3$. It turned out that a few of the structures he found did not actually satisfy the constraint of not distorting the octahedra.[15] For the RP214 systems the two principal approaches to this problem which have been used are a) a direct enumeration of likely structures[16] and b) the use symmetry.[17] This last approach utilizes a very useful computer program[18] to generate the isotropy subgroups of Ref. 19. In this way Hatch *et al.* [17] gave a listing for the RP214 structure of possible phase transitions involving distortions at various high symmetry wave vectors. This listing was shown to be consistent with the revised results of method a).[17] This important work has stood unquestioned for over a decade.[20] Here we show that most of structures listed in Refs. 17 and 20 for the RP214 systems are inconsistent with the constraint of rigid octahedra. To implement this constraint, we assume that the spring constants for distortion of the octahedra are larger than the other spring constants of the lattice by a factor of λ . Most of our results are obtained to leading order in $1/\lambda$, which we regard as an expansion parameter. This constraint

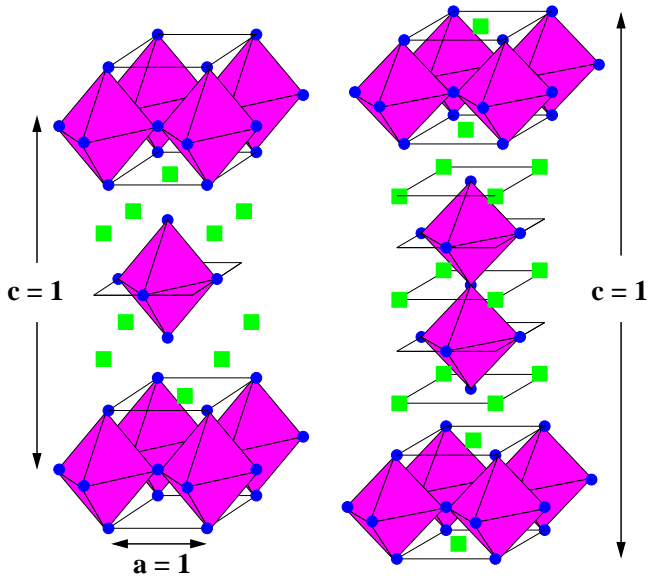


FIG. 1: (Color online) The high symmetry (body centered tetragonal) parent structure of A_2BO_4 (left) and $A_3B_2O_7$ (right). The green squares are A ions. The B ions are at the centers of the oxygen (blue dots) octahedra.

causes the quartic terms in the Landau free energy to assume a form which is less general than allowed by symmetry.[21] In some cases this constraint causes us to reject structures which have undistorted sublattices, a situation which is counterintuitive, since it is analogous to having a magnetic system simultaneously having ordered and disordered sublattices. Even for structures we our analysis allows, it is inevitable that in the structural phase transition the octahedra will undergo small (of order $1/\lambda$) distortions, which are observed.[22]

Briefly this paper is organized as follows. In Sec. II we enumerate the high symmetry wave vectors of the distortions we will consider and we discuss the role of the quartic terms in the Landau expansion in determining the detailed nature of the distortions. Here we also develop the nonlinear constraint induced by the rigidity of the octahedra. In Sec. III we apply these ideas to enumerate the possible structures which are allowed via a single phase transition involving a distortion at these high symmetry wave vectors for the RP214 structure. In Sec. IV we extend the treatment to the analogous RP327 ($A_3B_2C_7$) bilayer system. In Sec. V we use our results for $n = 1$ and $n = 2$ RP systems to obtain results for the RP systems $A_{n+1}B_nC_{3n+1}$ consisting of n -layer slabs (with n finite). In Sec. VI we discuss and summarize our results.

II. GENERAL PRINCIPLES

A. OVERVIEW

We will analyze possible distortions from the parent tetragonal system using a Landau-like formulation in which we write the free energy F as

$$F = \frac{1}{2} \sum_{k,l} A_{k,l}(T) X_k X_l + \mathcal{O}(X^4), \quad (1)$$

where X_k is a component of an ionic displacement. A structural phase transition occurs at a temperature T_0 when an eigenvalue of the matrix \mathbf{A} becomes zero. (For $T > T_0$ all the eigenvalues of \mathbf{A} are positive.) If the zero (critical) eigenvalue is N -fold degenerate, then for T near T_0 one has

$$F \sim \frac{a}{2} (T - T_0) \sum_{k=1}^N Q_k^2, \quad (2)$$

where Q_k is the amplitude of the k th linear combination of X 's given by the k th critical eigenvector of \mathbf{A} . As we shall see, higher order (in Q) corrections to the free energy in the cases of interest involve only even powers of the Q 's.

As is customary (*e. g.* see Ref. 17), we will restrict attention to the cases when Q is a superposition of displacements associated with the star of the high symmetry wave vectors $\mathbf{X} = (1/2, 1/2, 0)$, of $\mathbf{N} = (1/2, 0, 1/2)$, or of

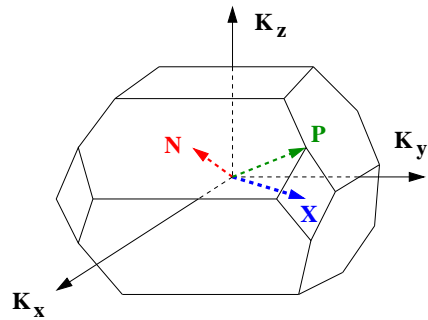


FIG. 2: (Color online) The first Brillouin zone for RP systems. There are two inequivalent $X = (1/2, 1/2, 0)$ points, four inequivalent N points, and two inequivalent P points. (Wave vectors are “equivalent” if their difference involves an integer number of reciprocal lattice vectors \mathbf{G} .)

$\mathbf{P} = (1/2, 1/2, 1/2)$. [23] These vectors are on faces of the first Brillouin zone as shown in Fig. 2. The reciprocal lattice vectors are

$$\begin{aligned} \mathbf{G}_1 &= (-1, 1, 1), & \mathbf{G}_2 &= (1, -1, 1), \\ \mathbf{G}_3 &= (1, 1, -1), & & \end{aligned} \quad (3)$$

Instead of dealing with irreducible representations (irreps), we will develop the free energy for the most general structure which can be constructed using the angular distortions at the wave vectors of the star of \mathbf{X} , \mathbf{N} , or \mathbf{P} .

To see how the form of the fourth order potential affects possible structural distortions, consider a system with two order parameters Q_1 and Q_2 related by symmetry, for which the free energy assumes the form

$$F = (T - T_0)[Q_1^2 + Q_2^2] + u[Q_1^2 + Q_2^2]^2 + vQ_1^2Q_2^2 \quad (4)$$

up to fourth order in Q with $u > 0$. As the temperature is lowered through the value T_0 the nature of the ordering depends on the sign of v . (See the phase diagram of Fig. 3.) If v is positive, then ordering has either Q_1 or Q_2 zero. If $-4u < v < 0$, ordering occurs with $|Q_1| = |Q_2|$. At the multicritical point [24,25] where v is zero (and also a similar sixth order anisotropy vanishes) one can have ordering in an arbitrary direction of order parameter (Q_1 - Q_2) space. Alternatively, analysis of terms of higher order than Q^4 shows that in extreme limits ordering can occur in an arbitrary direction in Q_1 - Q_2 space. Note that if we invoke *only* the symmetry properties of the system, there is no constraint on the parameters u and v , in which case the analysis of Ref. 17 would apply. However, as we will explain below, the picture of the lattice as consisting of oxygen octahedra implies a special form of the quartic terms with $u > 0$ and $v = -2u$, so that in most cases only structures with $|Q_1| = |Q_2|$ will actually occur.

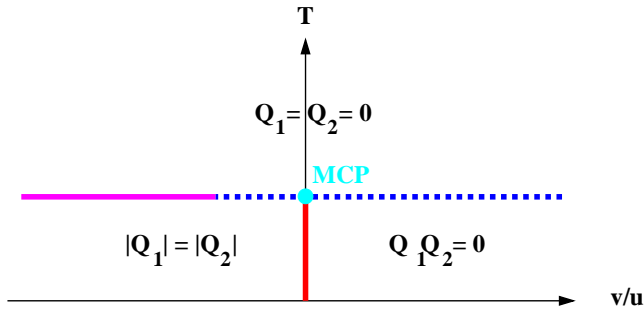


FIG. 3: (Color online) The mean-field phase diagram[25] (schematic) for the free energy of Eq. (4), showing the multicritical point (MCP) at $v = 0$. The dashed line indicates a continuous phase transition and the solid line a discontinuous one.

B. Octahedral Constraint

We now discuss the possible distorted configurations as constrained by the rigidity of the oxygen (or C ion) octahedra. In describing the distortions we use a notation similar to that of Ref. 17 and 20 which we deem more convenient for the RP systems than the widely used Glazer notation[14] for pseudocubic perovskites. For a single RP layer, we will first consider the rotation of octahedra through an angle 2θ about the tetragonal axis. Giving the angle of rotation of one octahedron at the origin fixes the rotation angles of all other octahedra in this layer. In the Glazer notation this would be specified as $a^0a^0b^+$ or $a^0a^0b^-$, where the superscripts 0 indicate zero rotation about the axes x and y , and b (implicitly equal to 2θ) is the rotation angle about the third (z) axis. The superscript $+$ or $-$ on b tells how the angle varies as we move from one layer perpendicular to z to the next layer. Here, since there is only one layer, this superscript is meaningless. More generally, for RP systems we have two slabs to consider, there would be two sets of Glazer symbols, one for each slab. However, we will give a simpler symbol which applies when the star of the wave vector is specified. (The Glazer symbol implicitly specifies the wave vector by the array of superscripts.)

For a rotation about the tetragonal z axis, the situation is that shown in Fig. 4. There one sees that a vertex common to two adjacent octahedra would, if the vertices were considered to be separate vertices for the two octahedra, become two closely, but distinct, separated points. In order to recover the common vertex, the two points would have to coalesce, which would require octahedral distortions of $\Delta_x/2$ and $\Delta_y/2$. However, it is possible for the lattice to relax, so that this mode would take place *without* any distortion of the octahedra. This relaxation involves microscopic strains along the x and y axes, to account for the Δ displacements. In the presence of microscopic strains ϵ_{xx} and ϵ_{yy} , one has for RP214

$$\Delta_{x,n} = a[2\theta_n^2 + \epsilon_{xx}],$$

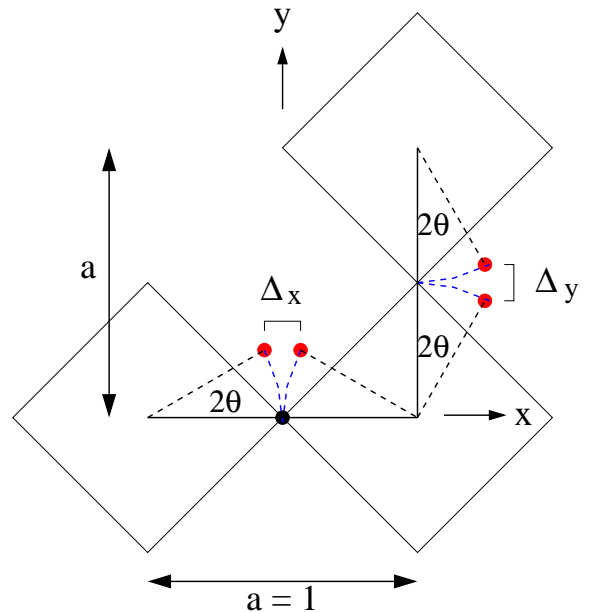


FIG. 4: (Color online) The octahedral constraint for interlocking θ -rotations about the tetragonal z axis. Here $\Delta_x = \Delta_y = 2a\theta^2$, where Δ_α is the mismatch that has to be absorbed either by a distortion of the octahedron or by a macroscopic strain when the octahedron is undistorted.

$$\Delta_{y,n} = a[2\theta_n^2 + \epsilon_{yy}], \quad (5)$$

where $\Delta_{\alpha,n}$ is the value of Δ_α for the n th slab and θ_n is the value of θ for the n th of the 2 slabs in the RP214 system. Therefore for RP214 the free energy per octahedron for the octahedrally constrained θ -rotated structure contains the term

$$F(\theta_1, \theta_2) = c_\theta a^2 \lambda \sum_{k=1}^2 \left[(2\theta_k^2 + \epsilon_{xx})^2 + (2\theta_k^2 + \epsilon_{yy})^2 \right] \quad (6)$$

where we have introduced the expansion parameter λ which is the ratio of the stiffness coefficient for distorting an octahedron to other stiffness coefficients of the lattice and c_θ , and below c_ϕ , are constants of order unity. Most of our results will be carried only to leading order in $1/\lambda$. Corrections higher order in $1/\lambda$ are discussed in the Appendix. Note that at order $1/\lambda$ it is inevitable that the octahedra will in fact be distorted.

We need to generalize Eq. (6) to allow for the rotation of octahedra about the tetragonal x and y axes. In the seminal work of Ref. 14 we are reminded that the group of rotations is nonabelian, i. e. rotations about different axes do not commute with one another. Here we discuss a simple nonlinear treatment of small rotations. We define the orientation of an octahedron by three variables, θ , ϕ_x , and ϕ_y which correspond to small rotations about the tetragonal axes.[26] These three variables correspond to the three Euler angles needed to specify the orientation of a rigid body when the rotation from the undistorted state is small. This situation is somewhat similar to the

spin wave expansion in which one introduces transverse spin components to describe the rotation of a three dimensional spin. A simple way to deal with this situation is to express the orientation of the vectors from the center of the octahedron to the equatorial vertices in terms of their transverse displacements as

$$\begin{aligned}\mathbf{r}_1 &= \left(\sqrt{1/4 - y_1^2 - z_1^2}, y_1, z_1 \right), \\ \mathbf{r}_2 &= \left(x_2, \sqrt{1/4 - x_2^2 - z_2^2}, z_2 \right), \\ \mathbf{r}_3 &= \left(-\sqrt{1/4 - y_3^2 - z_3^2}, y_3, z_3 \right), \\ \mathbf{r}_4 &= \left(x_4, -\sqrt{1/4 - x_4^2 - z_4^2}, z_4 \right),\end{aligned}\quad (7)$$

where \mathbf{r}_1 , \mathbf{r}_2 , \mathbf{r}_3 , and \mathbf{r}_4 are the rotated positions of the vertices whose respective original locations were $(1/2, 0, 0)$, $(0, 1/2, 0)$, $(-1/2, 0, 0)$, and $(0, -1/2, 0)$. Clearly, to retain the octahedral shape (with the center of mass fixed) we require that $\mathbf{r}_3 = -\mathbf{r}_1$ and $\mathbf{r}_4 = -\mathbf{r}_2$. We wish to incorporate the octahedral constraint to leading order in the transverse displacements. This constraint leads to

$$\begin{aligned}|\mathbf{r}_1 \pm \mathbf{r}_2|^2 &= \frac{1}{2} = \left(x_2 \pm \sqrt{\frac{1}{4} - y_1^2 - z_1^2} \right)^2 \\ &+ \left(y_1 \pm \sqrt{\frac{1}{4} - y_2^2 + z_2^2} \right)^2 + (z_1 \pm z_2)^2\end{aligned}\quad (8)$$

so that

$$0 = x_2 \sqrt{\frac{1}{4} - y_1^2 - z_1^2} + y_1 \sqrt{\frac{1}{4} - x_2^2 - z_2^2} + z_1 z_2. \quad (9)$$

This gives

$$0 = x_2 \left[\frac{1}{2} - y_1^2 - z_1^2 \right] + y_1 \left[\frac{1}{2} - x_2^2 - z_2^2 \right] + z_1 z_2 + \mathcal{O}(q^5),$$

where q is one or more of the variables. Thus

$$\frac{x_2 + y_1}{2} = -z_1 z_2 + x_2(y_1^2 + z_1^2) + y_1(x_2^2 + z_2^2) + \mathcal{O}(q^5) \quad (10)$$

We transform from the variables x_2 and y_1 to θ and $\delta\theta$:

$$x_2 = -\theta + \delta\theta, \quad y_1 = \theta + \delta\theta, \quad (12)$$

so that

$$\begin{aligned}\delta\theta &= -z_1 z_2 + [-\theta + \delta\theta][(\theta + \delta\theta)^2 + z_1^2] \\ &+ [\theta + \delta\theta][(-\theta + \delta\theta)^2 + z_2^2] + \mathcal{O}(q^5),\end{aligned}\quad (13)$$

which gives

$$\delta\theta = -z_1 z_2 + \theta(z_2^2 - z_1^2) + \mathcal{O}(q^4) \quad (14)$$

To make contact with the body of the paper replace z_1 by ϕ_x and z_2 by ϕ_y , to get

$$\begin{aligned}x_2 &= -\theta - \phi_x \phi_y + \theta(\phi_y^2 - \phi_x^2) + \mathcal{O}(q^4) \\ y_1 &= \theta - \phi_x \phi_y + \theta(\phi_y^2 - \phi_x^2) + \mathcal{O}(q^4) \\ x_1 &= \frac{1}{2} - y_1^2 - z_1^2 = \frac{1}{2} - \phi_x^2 - \theta^2 + 2\theta\phi_x\phi_y + \mathcal{O}(q^4) \\ y_2 &= \frac{1}{2} - x_2^2 - z_2^2 = \frac{1}{2} - \phi_y^2 - \theta^2 - 2\theta\phi_x\phi_y + \mathcal{O}(q^4)\end{aligned}\quad (15)$$

One sees that in terms of the variables θ , ϕ_x , and ϕ_y , the actual positions of the vertices are given by power series expansion in these variables, the lowest term of which identifies these variables directly with the corresponding displacements. (Of course, this expansion is only useful if the variables are small.) We can use these variables to analyze the symmetry of the free energy. In calculating scattering cross sections one must, of course, use the actual positions of the ions given by their nonlinear expansion, such as that in Eq. (15) or in Fig. 5, below.

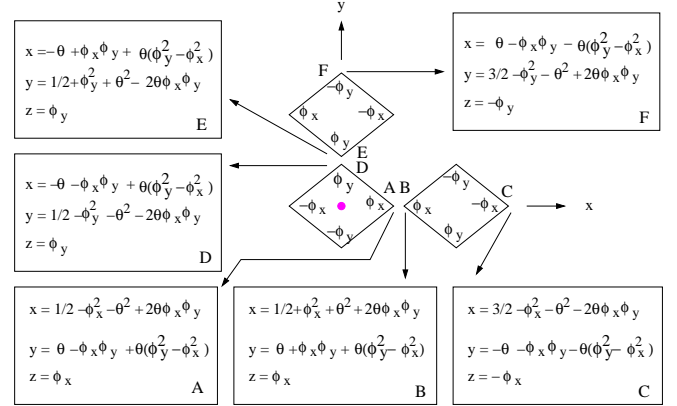


FIG. 5: (Color online) The displacements of the vertices for the star of \mathbf{X} including nonlinear contributions. The displacements of the lower left octahedron at the origin are given in terms of the expansion parameters of Eq. (15). The ϕ parameters at each vertex are shown. The θ displacements are only given in the formulas. Because the wave vectors of the star of \mathbf{X} are $(1/2, 1/2, 0)$ and $(1/2, -1/2, 0)$, the displacement of vertex C is related to that of vertex A by changing the signs of all the order parameters. The displacement of vertex F is obtained similarly from vertex D. The displacement of vertex B is obtained from that of vertex C by inversion about $(1, 0, 0)$ and that of vertex E from that of vertex F by inversion about $(0, 1, 0)$. The origin is indicated by the filled magenta circle.

In Fig. 5 we identify the displacements of the vertices for the star of \mathbf{X} . From this figure we obtain the mismatch of the vertex when considered to be two independent vertices of adjacent octahedra to be

$$\begin{aligned}x_B - x_A &= 2\phi_x^2 + 2\theta^2 + \frac{\partial u_x}{\partial x} \\ y_B - y_A &= 2\phi_x \phi_y + \frac{\partial u_y}{\partial x},\end{aligned}$$

$$\begin{aligned}
y_E - y_D &= 2\phi_y^2 + 2\theta^2 + \frac{\partial u_y}{\partial y}, \\
x_E - x_D &= 2\phi_x\phi_y + \frac{\partial u_x}{\partial y},
\end{aligned} \tag{16}$$

with corrections at order q^4 . Here $u(\mathbf{r})$ is the displacement field whose derivatives give rise to the strain tensor. Thus, for the star of \mathbf{X} we have

$$\begin{aligned}
F(\phi_{x,k}, \phi_{y,k}, \theta_k) &= c_\theta a^2 \lambda \sum_{k=1}^2 \left[(2\phi_{x,k}^2 + 2\theta_k^2 + \epsilon_{xx})^2 \right. \\
&\quad \left. + (2\phi_{y,k}^2 + 2\theta_k^2 + \epsilon_{yy})^2 \right] \\
&\quad + c_\phi a^2 \lambda \sum_{k=1}^2 (2\phi_{x,k}\phi_{y,k} + \epsilon_{xy})^2,
\end{aligned} \tag{17}$$

where $\epsilon_{xy} = [\partial u_x / \partial y + \partial u_y / \partial x] / 2$. Note that it is necessary to invoke a macroscopic strain to obtain a free energy of distortion which does not involve distorting the octahedra.[14,15] Coupling the θ or ϕ variables to a translational phonon will not bring all the octahedra along an axis closer together.

One might argue that ‘‘Constraining the form of the free energy departs ... from the accepted way of using symmetry in this theory. Any author is certainly free to postulate a modified free energy and derive consequences but the general appeal of this approach is then limited ...’’[27] The reason this objection is invalid is that our treatment is predicated on the fact that these RP systems consist of rigid octahedra. (This assumption of rigidity has been accepted by the research community for several decades and is supported by recent first principles calculations.[6,28–30]) One can imagine raising the temperature sufficiently or reducing the internal force constants so as to violate our assumption that the quartic potential due to intraoctahedral interactions dominates the quadratic terms in the Landau expansion. We refer to this limit as the limit of ‘‘octahedral melting.’’ For the RP perovskites, this limit is clearly irrelevant in practicality. But in perovskites, such as RP214, it is the geometry of the metal-oxygen bonds that leads to the rigidity of the octahedron. To ignore this physics and rely solely on symmetry (as implied by Ref. 27) is not sensible. To summarize: if it is legitimate to consider the system as consisting of rigid octahedra (as is the case for the RP perovskites), then the elastic energy quartic in the ionic displacements is dominated by coupling terms which arise from the distortion of individual octahedra. Note that the octahedra do not need to be infinitely rigid for our argument to be valid. They only need to be rigid enough that the parameters of the quartic potential are not very different from those for rigid octahedra.

III. RP214 STRUCTURES

A. The star of \mathbf{X}

As mentioned, we will develop a Landau expansion for RP214 structures associated with the star of the wave vector, \mathbf{X} , which includes $\mathbf{X}_1 = (1/2, 1/2, 0)$ and $\mathbf{X}_2 \equiv (1/2, -1/2, 0)$ providing that the octahedra rotate as constrained by their shared vertex. (See Fig. 6). In the $z = 0$ plane both \mathbf{X}_1 and \mathbf{X}_2 each imply that all angular variables alternate in sign as one moves between nearest neighbors. This fact fixes the values of all the ϕ 's and θ 's in the $z = 0$ plane in terms of the values for the octahedron labeled A in Fig. 6. If we had only the wave vector \mathbf{X}_1 , then the variables for octahedron B would be the negatives of those for octahedron A and the variables of octahedron C would be identical to those for octahedron A. If we had only the wave vector \mathbf{X}_2 then the variables for octahedra B and C would be reversed from what they were for wave vector \mathbf{X}_1 . Thus, if we have a linear combination of the two wave vectors, the orientational state for the plane $z = 1/2$ is characterized by assigning arbitrary values to the variables of octahedron B relative to which the values of all the other variables in that plane are fixed. Thus Fig. 6 gives the most general structure associated with the star of \mathbf{X} .

Therefore we write the elastic free energy for the RP214 structure of Fig. 6 for the star of \mathbf{X} as

$$\begin{aligned}
F(\phi_{x,k}, \phi_{y,k}, \theta_k) &= c_\theta a^2 \lambda \sum_{k=1}^2 \left[(2\phi_{x,k}^2 + 2\theta_k^2 + \epsilon_{xx})^2 \right. \\
&\quad \left. + (2\phi_{y,k}^2 + 2\theta_k^2 + \epsilon_{yy})^2 \right] \\
&\quad + c_\phi a^2 \lambda \sum_{k=1}^2 (2\phi_{x,k}\phi_{y,k} + \epsilon_{xy})^2 \\
&\quad + F_2 + F_4 + F_\epsilon + F_{2,\epsilon},
\end{aligned} \tag{18}$$

where the first terms come from Eq. (17) and last line contains terms of order λ^0 . Here F_2 (F_4) is the free energy quadratic (quartic) in the angles θ and ϕ , F_ϵ is the strain free energy at quadratic order, and $F_{2,\epsilon}$ is the rotation-strain coupling which is quadratic in the rotation variables and linear in the strains. Here we ignore quadratic terms involving modes which distort the octahedra, since they will not be activated. Also, as we shall see, terms coupling ϕ and θ variables such as $\lambda\theta_k^2(\phi_{x,k}^2 + \phi_{y,k}^2)$ do not affect the results because θ and ϕ are not simultaneously critical.

The free energy has to be invariant under all the symmetry operations of the ‘‘vacuum,’’ which, in this case, is the parent tetragonal structure. Accordingly, in Table I we give the effect of symmetry operations on the variables appearing in Eq. (18). Here and below, because of the octahedral constraint quartic terms of the form $\theta_1^2\theta_2^2$, $\phi_{x,1}^2\phi_{y,2}^2 + \phi_{x,2}^2\phi_{y,1}^2$, and $\phi_{x,1}\phi_{y,1}\phi_{x,2}\phi_{y,2}$ which are allowed by symmetry (see Table I) do not appear at order λ . (But, of course, they are present at order λ^0 . Only

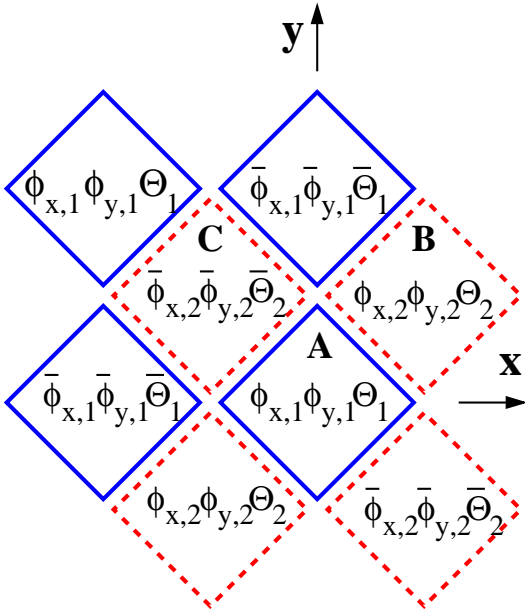


FIG. 6: (Color online) The structure of corner-sharing octahedra for the star of $\mathbf{X} \equiv (1/2, 1/2, 0)$ and $\mathbf{P} \equiv (1/2, 1/2, 1/2)$. The solid squares are the cross sections of octahedra in the $z = 0$ plane and the dashed squares are in the $z = 1/2$ plane. For clarity the octahedra are slightly separated instead of sharing vertices. Here ϕ_x means that the $+x$ vertex moves up by an amount ϕ_x and the $-x$ vertex moves down by an amount ϕ_x and similarly for ϕ_y . Also 2θ is the angle of rotation about the z axis. Here and below \bar{Q} denotes $-Q$. For \mathbf{X} the structure is invariant under $z \rightarrow z+1$. For \mathbf{P} the variables change sign under $z \rightarrow z+1$. The octahedral labels A, B, and C are needed for the discussion in the text.

quartic terms which arise from the octahedral constraint at a single vertex can appear at order λ .) Using Table I, we see that the quadratic terms which are invariant under the symmetry operations which leave the reference tetragonal structure invariant are

$$\begin{aligned}
 F_2 &= \alpha[\phi_{x,1}^2 + \phi_{y,1}^2 + \phi_{x,2}^2 + \phi_{y,2}^2] \\
 &\quad + 2\beta[\phi_{x,1}\phi_{y,2} + \phi_{x,2}\phi_{y,1}] + \gamma[\theta_1^2 + \theta_2^2] \\
 &\equiv \frac{1}{2}[\alpha - \beta] [(\phi_{x,1} - \phi_{y,2})^2 + (\phi_{x,2} - \phi_{y,1})^2] \\
 &\quad + \frac{1}{2}[\alpha + \beta] [(\phi_{x,1} + \phi_{y,2})^2 + (\phi_{x,2} + \phi_{y,1})^2] + \gamma[\theta_1^2 + \theta_2^2]
 \end{aligned}$$

Also

$$F_\epsilon = \frac{1}{2} \sum_{i,j} C_{ij} \epsilon_i \epsilon_j, \quad (20)$$

in the Voigt notation[31] where $1 \equiv (x, x)$, $2 \equiv (y, y)$, etc. Similarly, we use Table I to write

$$\begin{aligned}
 F_{2\epsilon} &= [\epsilon_{xx} + \epsilon_{yy}] [a_1(\theta_1^2 + \theta_2^2) + a_2(\phi_{x,1}\phi_{y,2} + \phi_{x,2}\phi_{y,1}) \\
 &\quad + a_3(\phi_{x,1}^2 + \phi_{y,1}^2 + \phi_{x,2}^2 + \phi_{y,2}^2)] \\
 &\quad + \epsilon_{zz} [a_4(\theta_1^2 + \theta_2^2) + a_5(\phi_{x,1}\phi_{y,2} + \phi_{x,2}\phi_{y,1})]
 \end{aligned}$$

$$\begin{aligned}
 &+ a_6(\phi_{x,1}^2 + \phi_{y,1}^2 + \phi_{x,2}^2 + \phi_{y,2}^2) + a_7 \epsilon_{xy} \theta_1 \theta_2 \\
 &+ a_8 [\epsilon_{xx} - \epsilon_{yy}] [\phi_{x,1}^2 + \phi_{x,2}^2 - \phi_{y,1}^2 - \phi_{y,2}^2] \\
 &+ a_9 [\phi_{x,1}\phi_{y,1} + \phi_{x,2}\phi_{y,2}] \epsilon_{xy}. \quad (21)
 \end{aligned}$$

We will deal with F_4 when it is needed. We will give analysis of the above free energy which neglects fluctuations. Our model has some resemblance to that of Bean and Rodbell[32] except that the form of the free energy does not drive the system to a first order phase transition, at least within mean field theory. An interesting problem would be to give a renormalization group analysis like that of Bergmann and Halperin[33] to elucidate the effects of orientation-strain coupling on the structural transitions.

TABLE I: Effect of symmetry operations on the variables of the stars of $\mathbf{X} \equiv (1/2, 1/2, 0)$ and $\mathbf{P} \equiv (1/2, 1/2, 1/2)$ (shown in Fig. 6) and on the strain variables. Here \mathcal{R}_4 is a four-fold rotation about the tetragonal z -axis passing through the origin, m_d and m_z are mirrors that take x into y and z into $-z$, respectively and T is the translation $(1/2, 1/2, 1/2)$. These variables are odd under the translations $T_x = (1, 0, 0)$ and $T_y = (0, 1, 0)$. For the star of \mathbf{X} , $\xi = 1$ and for the star of \mathbf{P} , $\xi = -1$. Note that spatial inversion \mathcal{I} is implicitly included because $\mathcal{I} = \mathcal{R}_4^2 m_z$. [34] In the last line $\Omega \equiv \epsilon_{xx} - \epsilon_{yy}$.

	\mathcal{R}_4	m_d	m_z	T
$\phi_{x,1}$	$\phi_{y,1}$	$\phi_{y,1}$	$-\phi_{x,1}$	$\phi_{x,2}$
$\phi_{y,1}$	$-\phi_{x,1}$	$\phi_{x,1}$	$-\phi_{y,1}$	$\phi_{y,2}$
$\phi_{x,2}$	$-\phi_{y,2}$	$\phi_{y,2}$	$-\xi\phi_{x,2}$	$\xi\phi_{x,1}$
$\phi_{y,2}$	$\phi_{x,2}$	$\phi_{x,2}$	$-\xi\phi_{y,2}$	$\xi\phi_{y,1}$
θ_1	θ_1	$-\theta_1$	θ_1	θ_2
θ_2	$-\theta_2$	$-\theta_2$	$\xi\theta_2$	$\xi\theta_1$
ϵ_{xy}	$-\epsilon_{xy}$	ϵ_{xy}	ϵ_{xy}	ϵ_{xy}
Ω	$-\Omega$	$-\Omega$	Ω	Ω

The structural phase transitions which we are investigating arise when *one* of the channels becomes unstable, i. e. when γ or $\alpha - |\beta|$ passes through zero. (As in Ref. 17, we reject multicritical points where more than one channel simultaneously becomes unstable.)

1. θ distortion

For instance, when only γ becomes negative, then

$$\phi_{x,1} = \phi_{x,2} = \phi_{y,1} = \phi_{y,2} = 0, \quad (22)$$

so that

$$\begin{aligned}
 F(\theta) &= c_\theta a^2 \lambda \sum_{k=1}^2 [(2\theta_k^2 + \epsilon_{xx})^2 + (2\theta_k^2 + \epsilon_{yy})^2] \\
 &\quad - \frac{1}{2} |\gamma| [\theta_1^2 + \theta_2^2] + F_4(\theta) + F_\epsilon + F_{2,\epsilon}, \quad (23)
 \end{aligned}$$

where $F_4(\theta)$ are quartic terms in θ of order λ^0 . To leading order in $1/\lambda$, when $F(\theta)$ is minimized, one finds that

$$\epsilon_{xx} = \epsilon_{yy} = -2\theta_1^2 = -2\theta_2^2. \quad (24)$$

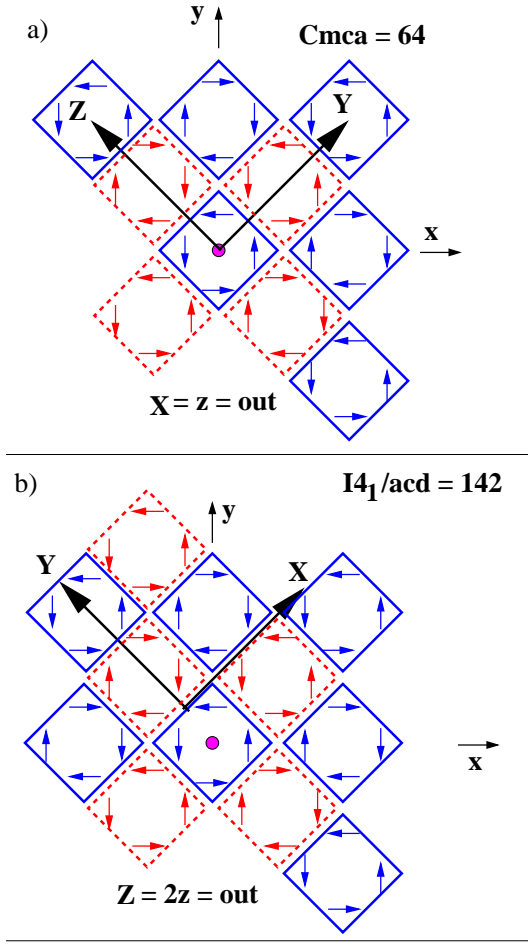


FIG. 7: (Color online) As Fig. 6. The structure of corner-sharing octahedra obtained by θ rotations either for $\mathbf{X} \equiv (1/2, 1/2, 0)$ (top) and $\mathbf{P} \equiv (1/2, 1/2, 1/2)$ (bottom). The arrows indicate the displacement of the oxygens in the equatorial plane. Here and in the figures below the original tetragonal axes are labeled by lower case letters and those of the distorted structure are labeled by capital letters. The magenta dot represents the tetragonal origin. In the top (bottom) panel $X = (0, 0, 1)_t$ ($Z = (0, 0, 2)_t$), where the subscript indicates that components are taken in the original tetragonal system. In the top (bottom) panel the distortion (changes sign) for $z \rightarrow z + 1$. In the top (bottom) panel the new origin is at $z = 0$ ($z = 3/4$).

(Corrections to this result at leading order in $1/\lambda$ are studied in Appendix A. In particular, there are no such corrections to the relation $\theta_1^2 = \theta_2^2$.) As we discuss in a moment, all choices of signs for the θ 's in Eq. (24) lead to equivalent structures, one of which is shown in Fig. 7a.

Now we identify the space group for the above θ distortion. The \mathbf{X} -structure has generators[35] ($X \pm 1/2, Y + 1/2, Z$), ($X, Y, Z + 1$), ($\bar{X}, \bar{Y}, \bar{Z}$), (X, \bar{Y}, \bar{Z}), and ($\bar{X} + 1/2, \bar{Y}, Z + 1/2$). In determining the space group from these generators,[36] it is useful to realize that the structures we find must form a subset of those listed in

Ref. 17. We thus identify the space group of the structure of Fig. 7a as D_{2h}^{18} or $Cmca$ (#64). $Cmca$ (64), one of the three θ -dependent structures of irrep X_2^+ for the star of \mathbf{X} which are listed in Ref. 17. However, we do not allow the other two structures of Ref. 17, the first of which (D_{2h}^9 or $Pbam$ =#55) has, according to Table III of Ref. 17, $|\theta_1| \neq |\theta_2|$, with $\theta_1\theta_2 \neq 0$ and the second of which (D_{4h}^5 or $P4/m3m$ =#127) has, according to Table III of Ref. 17, one sublattice distorted and the other not distorted, so that $\theta_1\theta_2 = 0$ (see Fig. 3). The problem with these structures is that to avoid distorting the octahedra we had to invoke a uniform strain which only relieves the distortions in the two slabs when the distortions in the two slabs are the same. Thus when $\theta_1^2 \neq \theta_2^2$, there is an unavoidable distortion energy of the octahedra of order λ .

Note also that the term in $F_{2\epsilon}$ proportional to $\epsilon_{xy}\theta_1\theta_2$ in combination with F_ϵ leads to

$$\epsilon_{xy} = -a_7\theta_1\theta_2/c_{44}, \quad (25)$$

This distortion is consistent with orthorhombic symmetry and with the orientation of the orthorhombic axes shown in Fig. 7. Rotating the crystal by 90° (\mathcal{R}_4) changes the sign of $\theta_1\theta_2$ and thus changes the sign of ϵ_{xy} , as one would expect.

In comparison to other ordering transitions we can make an analogy between the order parameters which govern the distortion from the parent tetragonal phase and the order parameters in, say, a magnetic system. In this formulation the distortion of the parent lattice in perovskites is analogous to the development of long-range magnetic order. Having a distortion only within one sublattice of the RP system is thus analogous to having magnetic order only on some sublattices. Although one can have ordered systems which have some disordered components, they differ from the present case. For instance, the orientational phase II of solid methane (CD_4) consists of a unit cell having six orientationally ordered methane molecules and two completely disordered molecules.[37] In that case, the site symmetry of the disordered molecules is high enough that the effective field from the ordered molecules vanishes. Furthermore, the interaction energy E between two disordered molecules is much less than kT , even at the lowest temperature at which phase II exists, so that they do not cooperatively order. Superficially, the situation here is similar to that for solid methane. For instance, suppose one builds up the distorted structure plane by plane for wave vectors in the star of \mathbf{X} or \mathbf{P} . The first plane would have $\theta = \theta_0$, say. Moving to the second plane we note a frustration due to the four-fold rotation, \mathcal{R}_4 which implies that the energy is invariant against changing the sign of θ_2 . (Table I indicates that \mathcal{R}_4 leaves θ_1 fixed but takes θ_2 into $-\theta_2$.) If one considers the third plane, there is no analogous frustration. One will have $\theta_3 = \pm\theta_1$, the sign depending on the weak interaction between octahedra in plane #1 and those in plane #3. More generally, $\theta_{n+2} = \sigma\theta_n$, where σ can be either $+1$ or -1 . As in quasi-

two dimensional systems, as the temperature at which the distortion becomes unstable is approached, two dimensional correlations will become significant and then even a weak coupling in the third dimension will lead to three dimensional long-range order at a single phase transition. This situation is reminiscent of the decoupling of magnetic sublattices in the bcc antiferromagnet.[38,39] The point is that if the distortion order parameter becomes nonzero in, say, the even numbered planes, the mechanism that led to this order would also apply to the odd numbered planes, which would then also distort at the same time. The distorting of both sublattices of octahedra could only be avoided if simultaneous distortions were strongly disfavored by the form of the quartic potential (*i. e.* if v of Eq. (4) were positive.) This possibility seems unlikely and indeed our analytic treatment of the octahedral constraint indicates that this scenario does not occur for large λ .

2. ϕ distortions

Now drop the θ variables, so that[40] the ϕ -dependent free energy for the star of \mathbf{X} is

$$F(\phi) = c_\theta a^2 \lambda \sum_{k=1}^2 \left[(2\phi_{x,k}^2 + \epsilon_{xx})^2 + (2\phi_{y,k}^2 + \epsilon_{yy})^2 \right] \\ + [(\alpha - \beta)/2] [(\phi_{x,1} - \phi_{y,2})^2 + (\phi_{x,2} - \phi_{y,1})^2] \\ + [(\alpha + \beta)/2] [(\phi_{x,1} + \phi_{y,2})^2 + (\phi_{x,2} + \phi_{y,1})^2] \\ + c_\phi a^2 \lambda \sum_{k=1}^2 (2\phi_{x,k}\phi_{y,k} + \epsilon_{xy})^2 + F_4(\phi), \quad (26)$$

where $F_4(\phi)$ are the terms quartic in ϕ which are proportional to λ^0 . When $F(\phi)$ is minimized for large λ , we get

$$\epsilon_{xx} = -2\phi_{x,1}^2 = -2\phi_{x,2}^2 \quad \Rightarrow \quad \phi_{x,2} = \pm\phi_{x,1}, \quad (27)$$

$$\epsilon_{yy} = -2\phi_{y,1}^2 = -2\phi_{y,2}^2 \quad \Rightarrow \quad \phi_{y,2} = \pm\phi_{y,1}, \quad (28)$$

and

$$\epsilon_{xy} = -2\phi_{x,1}\phi_{y,1} = -2\phi_{x,2}\phi_{y,2}. \quad (29)$$

There are four possible directions of the ordering vector $\Psi \equiv [\phi_{x,1}, \phi_{y,1}, \phi_{x,2}, \phi_{y,2}]$ depending on whether or not $\alpha - \beta$ becomes critical (zero) before $\alpha + \beta$ and the choice of signs in Eqs. (27) and (28). When $\alpha - \beta$ is critical (so that $\phi_{x,1} + \phi_{y,2} = \phi_{x,2} + \phi_{y,1} = 0$), then Ψ is proportional to either $a_1 = [11\bar{1}\bar{1}]$ or $b_1 = [\bar{1}\bar{1}11]$. If $\alpha + \beta$ is critical (so that $\phi_{x,1} - \phi_{y,2} = \phi_{x,2} - \phi_{y,1} = 0$), then Ψ is proportional to either $a_2 = [1111]$ or $b_2 = [\bar{1}\bar{1}\bar{1}\bar{1}]$. In each case, the two choices are equivalent:[41] $\mathcal{R}_4 b_n = a_n$. Figure 8 shows a representative of these solutions for each case.[42]

Finally, we identify the space groups of the structures of Fig. 8. The generators of b_1 are $(X \pm 1/2, Y +$

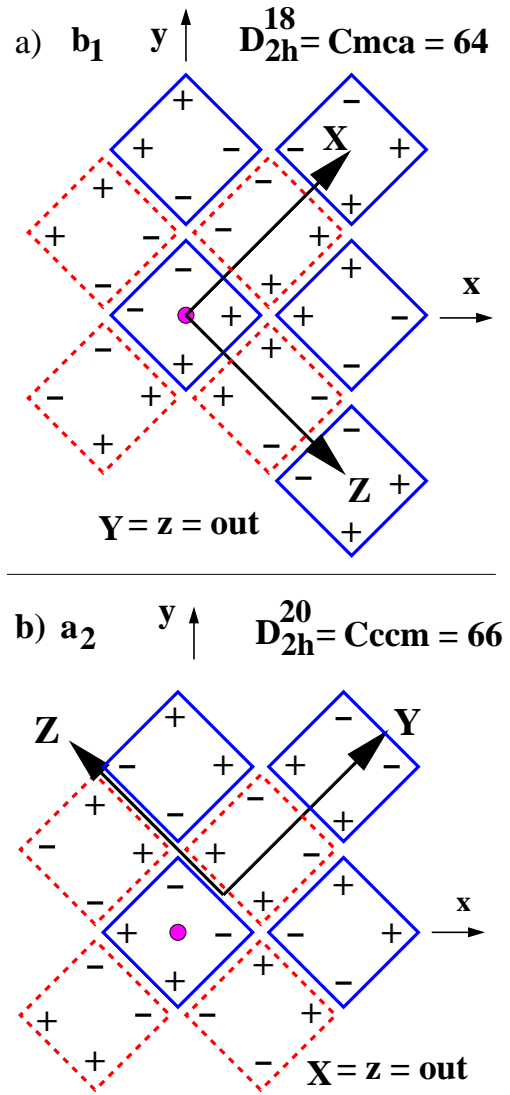


FIG. 8: (Color online) As Fig. 6 for the star of \mathbf{X} (with invariance under $z \rightarrow z + 1$). x , y , and z are the tetragonal axes and X , Y , and Z are the conventional lattice vectors after distortion. The filled magenta circle is the tetragonal origin. $\Psi \equiv [\phi_{x,1}, \phi_{y,1}, \phi_{x,2}, \phi_{y,2}] = [1\bar{1}\bar{1}\bar{1}]$ for a) and $[\bar{1}\bar{1}\bar{1}\bar{1}]$ for b).[42] The irreps are given in Table III. The new origin has $z = 0$ for a) and $z = 1/4$ for b). The third new axis vector is $[001]_t$ in terms of the original tetragonal coordinates.

$1/2, Z)$, $(X, Y, Z + 1)$, $(\bar{X}, \bar{Y}, \bar{Z})$, (X, \bar{Y}, \bar{Z}) , and $(\bar{X} + 1/2, \bar{Y}, 1/2 + Z)$ and those of a_2 are $(X \pm 1/2, Y + 1/2, Z)$, $(X, Y, Z + 1)$, $(\bar{X}, \bar{Y}, \bar{Z})$, (\bar{X}, \bar{Y}, Z) , and $(X, \bar{Y}, 1/2 + \bar{Z})$. From these generators we identify the space groups as indicated in Fig. 8. From Eq. (21) we see from the term in a_8 that $\epsilon_{xx} = \epsilon_{yy}$ for both these structures. The term in a_9 indicates that $\epsilon_{xy} \neq 0$, consistent with the orientation of the coordinate axes shown in Fig. 8.

Note that, in comparison to Ref. 17, our formulation does not allow the structures of space groups Pccn ($D_{2h}^{10} = \#56$) and Pnnn ($D_{2h}^2 = \#48$). From Table III of Ref. 17 one sees that Pccn has $\phi_{x,1} = \phi_{y,2} = a$ and $\phi_{y,1} =$

$\phi_{x,2} = b$, with $a \neq b$ and Pnnn has $\phi_{x,1} = -\phi_{y,2} = a$ and $\phi_{y,1} = -\phi_{x,2} = b$, with $a \neq b$. As before, to relieve the distortion of the octahedra via strains implies that the order parameters have the same magnitude on both sublattices. Similarly we do not allow space groups $P4_2/nm$ ($D_{4h}^{16} = \# 138$) and $P4_2/nmm$ ($D_{4h}^{12} = \# 134$) which have (in one setting) $\phi_{x,1} = \phi_{y,2} = 0$ and $|\phi_{x,2}| = |\phi_{y,1}|$. Our analysis of the space groups listed in Ref. 17 is summarized in Tables II and III.

TABLE II: Space groups of Ref. 17 for the stars if **X**, **N**, and **P** which we do not allow for RP214's. For the column headings "S" stands for the Schoenflies symbol, "H-M" stands for the short Hermann-Mauguin symbol as given in Ref. 8, and # is the number of the space group in Ref. 8. For otherwise identical space groups, the footnotes give the basis vectors of the unit cell in terms of the original tetragonal coordinates. The irrep labels are from Ref. 17.

Irrep	S	#	H-M	S	#	H-M
X_2^+	D_{4h}^5	127	P_4/mbm	D_{2h}^9	55	Pbam
X_3^+	D_{2h}^{10}	56	Pccn	D_{4h}^{16}	138	$P4_2/nm$
X_4^+	D_{2h}^2	48	Pnnn	D_{4h}^{12}	134	$P4_2/nmm$
N_1^+	C_{2h}^1	10	$P2/m$	C_i^1	2	$P\bar{1}^{***}$
N_1^+	D_{2h}^{28}	74	Imma*	D_{2h}^{25}	71	Immm
N_1^+	C_{2h}^6	15	$C2/c$	C_{2h}^3	12	$C2/m^\dagger$
N_1^+	C_{2h}^3	12	$C2/m^{\dagger\dagger}$	D_{4h}^{19}	141	$I4_1/amd$
N_1^+	D_{2h}^{19}	65	Cmmm	D_{4h}^{17}	139	$I4/mmm$
P_4	D_{4h}^{18}	140	$I4/mmm$	D_{2d}^{10}	122	$I\bar{4}2d$
P_5	D_{2h}^{28}	74	Imma**	D_{2h}^{24}	69	Fmmm
P_5	S_2^2	82	$I\bar{4}$	C_{2v}^{22}	46	Ima2
P_5	C_{2v}^{19}	43	Fdd2	C_{2v}^{18}	42	Fmm2
P_5	D_2^9	24	$I2_12_12_1$	D_2^8	23	I222
P_5	D_2^7	22	F222	C_{2h}^6	15	$C2/c$
P_5	C_{2h}^3	12	$C2/m^{\dagger\dagger\dagger}$	C_2^3	5	$C2$

*: (200), (020), (002). **: (002), ($1\bar{1}0$), (110).
***: ($\bar{1}11$), ($\frac{1}{2}\bar{1}\frac{1}{2}$), (11 $\bar{1}$). †: (00 $\bar{2}$), ($\bar{2}20$), ($\bar{1}11$).
††: ($\bar{2}0\bar{2}$), (0 $\bar{2}0$), (0,0,2). †††: (020), (002), ($1\bar{1}0$).

B. The star of N

Similarly, we construct the most general structure for the star of **N** $\equiv (1/2, 0, 1/2)$ whose wave vectors are $\mathbf{N}_1 \equiv (1/2, 0, 1/2)$, $\mathbf{N}_2 = (-1/2, 0, 1/2)$, $\mathbf{N}_3 = (0, 1/2, 1/2)$, and $\mathbf{N}_4 = (0, -1/2, 1/2)$. To do this we use Fig. 9. Consider first the situation in the $z = 0$ plane. Note that ϕ_x has to alternate in sign as we move along x . This means that ϕ_x is associated with a linear combination of \mathbf{N}_1 and \mathbf{N}_2 distortions. Since $N_{1,y} = N_{2,y} = 0$, we see that ϕ_x must be independent of y . Similar reasoning indicates that ϕ_y alternates along y and is therefore associated with a linear combination of \mathbf{N}_3 and \mathbf{N}_4 distortions. Therefore ϕ_y is independent of x . These wave vectors do not support nonzero values of θ . We have thereby fixed all the values of the variables in the $z = 0$ plane in terms of

TABLE III: As Table II. Space groups of Ref. 17 for the stars of **X**, **N**, and **P** which we do allow for RP214's. Under "Var's" we give the variables active in the mode and under "Fig" we give the number of the illustrative figure.

Irrep	Var's	S	#	H-M	Fig
X_2^+	θ	D_{2h}^{18}	64	Cmca	7a
X_3^+	ϕ_x, ϕ_y	D_{2h}^{18}	64	Cmca	8a
X_4^+	ϕ_x, ϕ_y	D_{2h}^{20}	66	Cccm	8b
N_1^+	ϕ_y	C_{2h}^3	12	$C2/m^\dagger$	10b
N_1^+	ϕ_x, ϕ_y	C_{2h}^3	12	$C2/m^{\dagger\dagger}$	10c
N_1^+	ϕ_x, ϕ_y	C_i^1	2	$P\bar{1}^{***}$	10a
P_4	θ	D_{4h}^{20}	142	$I4_1/acd$	7b
P_5^*	ϕ_x, ϕ_y	D_{2h}^{26}	72	Ibam	11a
P_5^*	ϕ_x, ϕ_y	C_{2h}^6	15	$C2/c$	11c
P_5^*	ϕ_y	D_{2h}^{24}	70	Fddd	11b

†: ($0\bar{1}1$), (100), (011).

††: (002), (220), ($\frac{1}{2}\frac{1}{2}\frac{1}{2}$).

* The wave vector may be close to, but not exactly at, the star of **P**.

** : ($\bar{1}11$), ($1\bar{1}1$), (11 $\bar{1}$).

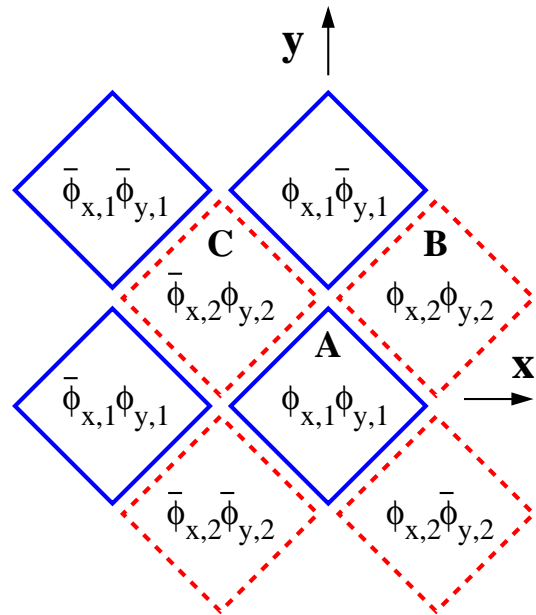


FIG. 9: (Color online) As Fig. 6. The structure of corner-sharing octahedra for the star of **N**. The variables change sign under $z \rightarrow z + 1$.

those of octahedron A. Now consider the situation in the $z = 1/2$ plane. Suppose we have a linear combination of \mathbf{N}_1 and \mathbf{N}_2 which gives rise to $\phi_{x,1}$ for octahedron A. If we had only \mathbf{N}_1 , then the variables for octahedron B would be $-\phi_{x,1}$ and $-\phi_{y,1}$, whereas if we had \mathbf{N}_2 , then these variables would be $\phi_{x,1}$ and $\phi_{y,1}$. As for the case

TABLE IV: As Table I, but for the RP327 variables of the star of $\mathbf{N} \equiv (1/2, 0, 1/2)$ (shown in Fig. 9). $T \equiv (1/2, 1/2, 1/2)$, $T_x \equiv (1, 0, 0)$, and $T_y \equiv (0, 1, 0)$. All variables are odd under $T_z \equiv (0, 0, 1)$.

	\mathcal{R}_4	m_d	m_z	T	T_x	T_y
$\phi_{x,1}$	$\phi_{y,1}$	$\phi_{y,1}$	$-\phi_{x,1}$	$\phi_{x,2}$	$-\phi_{x,1}$	$\phi_{x,1}$
$\phi_{y,1}$	$-\phi_{x,1}$	$\phi_{x,1}$	$-\phi_{y,1}$	$\phi_{y,2}$	$\phi_{y,1}$	$-\phi_{y,1}$
$\phi_{x,2}$	$\phi_{y,2}$	$\phi_{y,2}$	$\phi_{x,2}$	$\phi_{x,1}$	$-\phi_{x,2}$	$\phi_{x,2}$
$\phi_{y,2}$	$\phi_{x,2}$	$\phi_{x,2}$	$\phi_{y,2}$	$\phi_{y,1}$	$\phi_{y,2}$	$-\phi_{y,2}$

of the star of \mathbf{X} , we conclude that all the variables in the second layer are fixed in terms of the arbitrary variables of octahedron B, so that Fig. 9 characterizes the most general structure arising from the star of \mathbf{N} . The effect of symmetry operations on these variables is given in Table IV.

We need to establish the analog of Fig. 5 for the star of \mathbf{N} . First of all, here we can set $\theta = 0$. Also, note that for sites B and C, the sign of ϕ_y is reversed for the star of \mathbf{N} in comparison to that for the star of \mathbf{X} . For site A, \mathbf{r}_A for the star of \mathbf{N} is as in Fig. 5. However, now

$$\mathbf{r}_B = (1/2 + \phi_x^2, -\phi_x\phi_y, \phi_x). \quad (30)$$

Therefore $y_B - y_A = z_B - z_A = 0$ and $x_B - x_A = 2\phi_x^2$. Likewise, for site D Fig. 5 applies equally for the star of \mathbf{N} . However, for sites E and F the sign of ϕ_x is reversed for the star of \mathbf{N} from what it was for the star of \mathbf{X} . So

$$\mathbf{r}_E = (-\phi_x\phi_y, 1/2 + \phi_y^2, \phi_y), \quad (31)$$

so that $x_E - x_D = z_E - z_D = 0$ and $y_E - y_D = 2\phi_y^2$.

We now write the Landau expansion for the star of \mathbf{N} . Taking account of the symmetries of Table IV and the preceding discussion, we obtain the relevant terms in the free energy for the star of \mathbf{N} to be

$$\begin{aligned} F_N = c_\theta a^2 \lambda & \left[(2\phi_{x,1}^2 + \epsilon_{xx})^2 + (2\phi_{y,1}^2 + \epsilon_{yy})^2 \right. \\ & \left. + (2\phi_{x,2}^2 + \epsilon_{xx})^2 + (2\phi_{y,2}^2 + \epsilon_{yy})^2 \right] \\ & + \frac{\alpha}{2} [\phi_{x,1}^2 + \phi_{y,1}^2 + \phi_{x,2}^2 + \phi_{y,2}^2] + F_{2\epsilon} + F_4 \end{aligned} \quad (32)$$

where

$$\begin{aligned} F_4 = \frac{u}{4} & \left[(\phi_{x,1}^2 + \phi_{y,1}^2)^2 + (\phi_{x,2}^2 + \phi_{y,2}^2)^2 \right] \\ & + v (\phi_{x,1}^2 \phi_{y,1}^2 + \phi_{x,2}^2 \phi_{y,2}^2) + w (\phi_{x,1}^2 \phi_{x,2}^2 + \phi_{y,1}^2 \phi_{y,2}^2) \\ & + x (\phi_{x,1}^2 \phi_{y,2}^2 + \phi_{y,1}^2 \phi_{x,2}^2). \end{aligned} \quad (33)$$

To leading order in $1/\lambda$ the minima of F_N occur for

$$\begin{aligned} \epsilon_{xx} = -2\phi_{x,1}^2 = -2\phi_{x,2}^2 & \Rightarrow \phi_{x,2} = \pm\phi_{x,1} \\ \epsilon_{yy} = -2\phi_{y,1}^2 = -2\phi_{y,2}^2 & \Rightarrow \phi_{y,2} = \pm\phi_{y,1}. \end{aligned} \quad (34)$$

The quartic terms distinguish between these solutions. If $\phi_x^2 \equiv \phi_{x,1}^2 = \phi_{x,2}^2$ and similarly for ϕ_y , then we have

$$F_4 = 2(v - w + x)\phi_x^2\phi_y^2 + [w + (u/2)](\phi_x^2 + \phi_y^2)^2 \quad (35)$$

This indicates that we can have a structural phase transition into three classes of states. We can have a continuous phase transition into states of class A with $\phi_x^2 = \phi_y^2$ if $(v - w + x)$ is negative or into a state of class B with $\phi_x\phi_y = 0$ if $(v - w + x)$ is positive. In addition, we can have a phase transition to a state of class C in which ϕ_x and ϕ_y do not assume special values if the higher order terms cause the transition to be discontinuous. The next step is to determine which of these solutions are inequivalent, i. e. which are not related by a symmetry operation.[41]

We first show that all solutions of class A are equivalent to one another. Using the results given in Table IV we have that

$$(1 + \mathcal{R}_4 + \mathcal{R}_4^2 + \mathcal{R}_4^3) [1111] = [\{\mu\nu\}11], \quad (36)$$

where $\{\mu\nu\}$ indicates the set of μ, ν values, i. e. $\{\mu\nu\} = 11 + \bar{1}\bar{1} + \bar{1}1 + 1\bar{1}$. Then

$$T(1 + \mathcal{R}_4 + \mathcal{R}_4^2 + \mathcal{R}_4^3) [1111] = [\bar{1}\bar{1}\{\mu\nu\}] \equiv \Phi, \quad (37)$$

and finally

$$(1 + \mathcal{R}_4 + \mathcal{R}_4^2 + \mathcal{R}_4^3) \Phi = [\{\rho\tau\}\{\mu\nu\}], \quad (38)$$

where (apart from an arbitrary amplitude) the right-hand side of this equation includes all vectors of class A. In class A, $\phi_x^2 = \phi_y^2$, so that $\epsilon_{xx} = \epsilon_{yy}$ and we take $[\bar{1}\bar{1}\bar{1}\bar{1}]$ as its representative. The term in Eq. (21) proportional to a_9 indicates that $\epsilon_{xy} \neq 0$ for this structure.

Next we consider solutions of class B. From Table IV note that

$$[1 + \mathcal{R}_4^2][1 + T_x][1010] = \sum_{\mu\nu=\pm 1} [\mu 0\nu 0] \equiv \Phi. \quad (39)$$

and

$$\mathcal{R}_4\Phi = \sum_{\mu\nu=\pm 1} ([\mu 0\nu 0] + [0\mu 0\nu]). \quad (40)$$

The right-hand side includes all vectors of class B. We may take $[010\bar{1}]$ as the representative of class B.

Finally we consider solutions of class C, which are of the form $[x, y, \pm x, \pm y]$, where $|x| \neq |y|$ and both are nonzero. Using Table IV we write

$$m_d \mathcal{R}_4[x, y, x, y] = [x\bar{y}xy] \quad (41)$$

so that

$$[1 + m_z][1 + m_d \mathcal{R}_4][xyxy] = \sum_{\sigma_1=\pm 1} \sum_{\sigma_2=\pm 1} (\sigma_1 x, \sigma_2 y, x, y) \quad (42)$$

From this we conclude that all vectors of class C are equivalent to one another, and we take their representative to be $[\bar{x}y\bar{x}y]$.

Thus, in all, we have the three allowed space groups from the star of \mathbf{N} shown in Figs. 10 and 11: $[\bar{x}y\bar{x}y]$, $[010\bar{1}]$, and $[\bar{1}\bar{1}\bar{1}\bar{1}]$. As before, to determine the space

groups of the structures we use Figs. 10 and 11 to write down their generators. For $[\bar{x}y\bar{x}y]$ the generators are $(X+1, Y, Z)$, $(X, Y+1, Z)$, $(X, Y, Z+1)$, and $(\bar{X}, \bar{Y}, \bar{Z})$, which is C_i^1 ($P\bar{1} = \# 2$). For both $[010\bar{1}]$ and $[\bar{1}\bar{1}\bar{1}\bar{1}]$, the generators are $(X, Y, Z+1)$, $(X+1/2, Y+1/2, Z)$, $(X+1/2, Y-1/2, Z)$, $(\bar{X}, \bar{Y}, \bar{Z})$, and (\bar{X}, Y, \bar{Z}) which is C_{2h}^3 ($C2/m = \#12$). Although these two structures belong to the same space group, they are different because their unit cells are different (see Figs. 10 and 11).

In Table III (II) we list the structures which are (not) allowed. We only allow one of the eight structures for the irrep N_1^+ listed in Ref. 17 which occur via a discontinuous transition. In addition, Ref. 17 lists two space groups Cmmm (65) for which $\Psi = [1000]$ and I4/mmm(139) for which $\Psi = [1100]$. Both these are inconsistent with the fourth order terms arising from the rigid octahedral constraint. [I. e. they did not arise from Eq. (32)]. They are also counterintuitive in that they both describe states in which nonzero order parameters appear only on alternate planes. [Look back at the discussion below Eq. (24)].

C. The star of P

The star of \mathbf{P} consists of the vectors $\mathbf{P}_1 \equiv (1/2, 1/2, 1/2)$ and $\mathbf{P}_2 \equiv (1/2, -1/2, 1/2)$. The possible structures are identical to those for the star of \mathbf{X} , except that the variables change sign under $z \rightarrow z+1$ as indicated in Fig. 6. The transformation properties of these variables are given in Table I. The quartic terms are the same as for the star of \mathbf{X} . However, the quadratic terms differ because of the ξ factors that appear in Table I. The octahedral constraint assumes the same form as for the star of \mathbf{X} because the stars of \mathbf{X} and \mathbf{P} only differ in how the layers are stacked. Therefore for the star of \mathbf{P} we have

$$\begin{aligned}
F(\phi_{x,k}, \phi_{y,k}, \theta_k) = & c_\theta a^2 \lambda \sum_{k=1}^2 \left[(2\phi_{x,k}^2 + 2\theta_k^2 + \epsilon_{xx})^2 \right. \\
& \left. + (2\phi_{y,k}^2 + 2\theta_k^2 + \epsilon_{yy})^2 \right] \\
& + c_\phi a^2 \lambda \sum_{k=1}^2 (2\phi_{x,k}\phi_{y,k} + \epsilon_{xy})^2 \\
& + F_2 + F_4 + F_\epsilon + F_{2,\epsilon} . \quad (43)
\end{aligned}$$

1. θ distortions

We analyze these as before. In the channel where γ passes through zero, we have

$$\begin{aligned}
F(\theta) = & c_\theta a^2 \lambda \sum_{k=1}^2 \left[(2\theta_k^2 + \epsilon_{xx})^2 + (2\theta_k^2 + \epsilon_{yy})^2 \right] \\
& - \frac{1}{2} |\gamma| [\theta_1^2 + \theta_2^2] + F_4(\theta) + F_\epsilon + F_{2,\epsilon} , \quad (44)
\end{aligned}$$

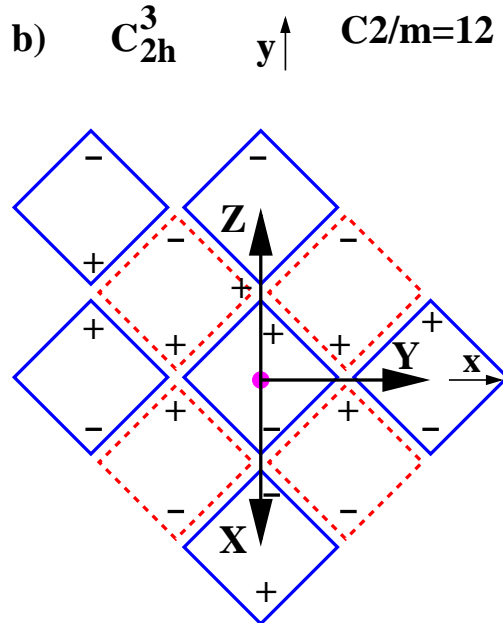
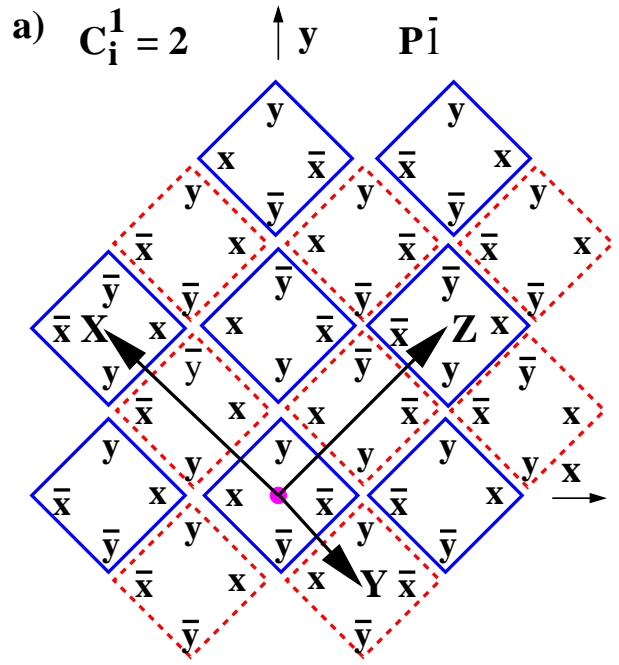


FIG. 10: (Color online) As Fig. 8 for the star of \mathbf{N} (with sign change under $z \rightarrow z+1$) for a) (class C) $[\bar{x}y\bar{x}y]$ and b) (class B) $[010\bar{1}]$. x , y and z are the tetragonal axes, and X , Y , and Z are $[(\bar{1}\bar{1}\bar{1}), (1/2, -1/2, 1/2), (11\bar{1})]$ in a) and $[(0\bar{1}\bar{1}), (100), (011)]$ in b). All the new origins are at $z = 0$.

so that $|\theta_1| = |\theta_2|$. This structure has the same degeneracy associated with the relative phase of even and odd layers that we saw for the previous θ structures (at the star of \mathbf{X}). Because $P_z = 1/2$, the only θ -dependent structure has $\theta_{n+2} = -\theta_n$. The other two structures

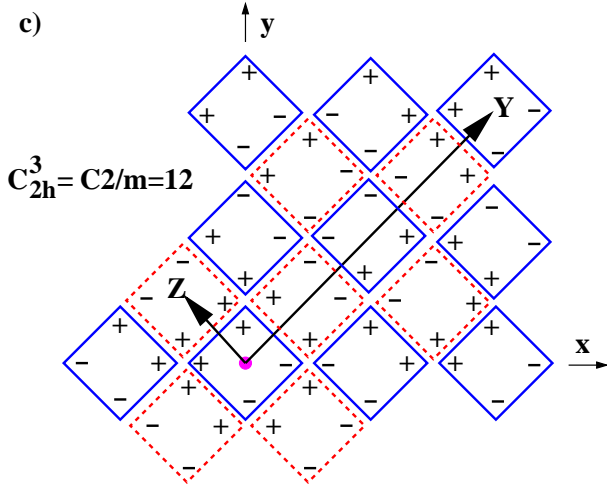


FIG. 11: (Color online) Continuation of Fig. 10. for c) (class A) $[\bar{1}\bar{1}\bar{1}]$. X , Y , and Z are $[(002),(220)(-1/2, 1/2, -1/2)]$. The new origins is at $z = 0$.

listed in Ref. 17 which have $|\theta_1| \neq |\theta_2|$ are not admissible due to the form of the term proportional to λ in Eq. (44). The allowed \mathbf{P} -structure, shown in Fig. 7b has generators $(X - 1/2, Y + 1/2, Z + 1/2)$, $(X + 1/2, Y - 1/2, Z + 1/2)$, $(X + 1/2, Y + 1/2, Z - 1/2)$, $(\bar{X}, \bar{Y}, \bar{Z})$, $(X, \bar{Y}, \bar{Z} + 1/2)$, and $(\bar{Y} + 1/4, X + 3/4, Z + 1/4)$, which is space group D_{4h}^{20} or $I4_1/acd$ (# 142).

2. ϕ distortions

Now consider the ϕ -dependent solutions which are associated with irrep P_5 according to Ref. 17. Note that all the subgroups from this irrep listed there and in Ref. 19 do not satisfy the Lifshitz condition. What this means is that the quadratic instability occurs at a wave vector that is not fixed by symmetry[43] (so that it can not be assumed to be at the star of \mathbf{P}). Accordingly, the wave vector can only be at the star of \mathbf{P} if the transition is discontinuous.

However, we can determine which structures with wave vectors either at or near the star of \mathbf{P} can be condensed. To do this, we simply ignore the Lifshitz criterion in our analysis of the free energy. For this purpose we consider the ϕ -dependent free energy which is

$$\begin{aligned}
 F = & c_\theta a^2 \lambda \sum_{k=1}^2 \left[(2\phi_{x,k}^2 + \epsilon_{xx})^2 \right. \\
 & \left. + (2\phi_{y,k}^2 + \epsilon_{yy})^2 \right] \\
 & + c_\phi a^2 \lambda \sum_{k=1}^2 (2\phi_{x,k}\phi_{y,k} + \epsilon_{xy})^2 \\
 & + \frac{1}{2} \alpha [\phi_{x,1}^2 + \phi_{y,1}^2 + \phi_{x,2}^2 + \phi_{y,2}^2]
 \end{aligned}$$

$$+ F_4 + F_\epsilon + F_{2,\epsilon} . \quad (45)$$

and we consider the phase transition which occurs when α passes through zero. For large λ we must have

$$\begin{aligned}
 \epsilon_{xx} &= -2\phi_{x,1}^2 = -2\phi_{x,2}^2 \\
 \epsilon_{yy} &= -2\phi_{y,1}^2 = -2\phi_{y,2}^2 \\
 \epsilon_{xy} &= -2\phi_{x,1}\phi_{y,1} = -2\phi_{x,2}\phi_{y,2} .
 \end{aligned} \quad (46)$$

Thus we have three classes of solutions: in class A we have $[1, 0, \pm 1, 0]$ and $[0, 1, 0, \pm 1]$. In class B we have $[11\sigma\sigma]$ and $[1\bar{1}\sigma\bar{\sigma}]$ with $\sigma = 1$, class C is like B, except that $0 < \sigma < 1$. These three classes are associated with the different minima of F_4 which assumes the same form as in Eq. (33). The analysis to show that all members of same class are actually equivalent follows the previous arguments, so we will not repeat it here. The three solutions are shown in Fig. 12. We take the representatives to be $[0\bar{1}0\bar{1}]$ for class A, $[\bar{1}\bar{1}\bar{1}]$ for class B, and $[xyxy]$ for class C.

As before, we identify the space groups of these solutions by determining the generators of the representatives shown in Fig. 12. For a) ($[0\bar{1}0\bar{1}]$) the generators are $[44]$ (X, Y, \bar{Z}) , $(X, \bar{Y}, \bar{Z} + 1/2)$, $(\bar{X}, \bar{Y}, \bar{Z})$, $(X - 1/2, Y + 1/2, Z + 1/2)$, $(X + 1/2, Y - 1/2, Z + 1/2)$, $(X + 1/2, Y + 1/2, Z - 1/2)$ and thus the space group is $Ibam$ ($D_{2h}^{26} = \#72$). For b) ($[\bar{1}\bar{1}\bar{1}]$) the generators are $(\bar{X} + 1/4, \bar{Y} + 1/4, Z)$, $(X, \bar{Y} + 1/4, \bar{Z} + 1/4)$, $(\bar{X}, \bar{Y}, \bar{Z})$, $(X, Y + 1/2, Z + 1/2)$, $(X + 1/2, Y, Z + 1/2)$, $(X + 1/2, Y + 1/2, Z)$, and thus the space group is $Fddd$ ($D_{2h}^{24} = \#70$). For c) ($[xyxy]$) the generators are $(\bar{X}, Y, \bar{Z} + \frac{1}{2})$, $(\bar{X}, \bar{Y}, \bar{Z})$, $(X + 1/2, Y + 1/2, Z)$, $(X - 1/2, Y + 1/2, Z)$, $(X, Y, Z + 1)$ and thus the space group is $C2/c$ ($C_{2h}^3 = \#15$). When the Lifshitz instability is resolved, these space groups give rise either to commensurate structures at the star of \mathbf{P} via a first order transitions or to structures having incommensurate wave vectors near the star of \mathbf{P} .

IV. RP327 STRUCTURES

In this section we perform the same analysis for the $n = 2$ RP systems $A_3B_2C_7$ which we call the RP327 systems. As shown in Fig. 1, these systems consist of two slabs. Each slab consists of two layers which we label a and b (or 1 and 2). If we fix the ϕ variables in layer a , the octahedral constraint fixes each ϕ variable in layer b to be the negative of its nearest neighbor in layer a . As a result each structure of the RP327 system is characterized by the same number of ϕ variables as its analog for the RP214 system. In contrast, since there is no such relation between the θ variables of layers a and b , we introduce variables $\theta_{n,x}$ to describe the rotation within the x th layer ($x = a, b$) of the n th slab ($n = 1, 2$), as shown in Fig. 14. The transformation properties of the variables are summarized in Table V.

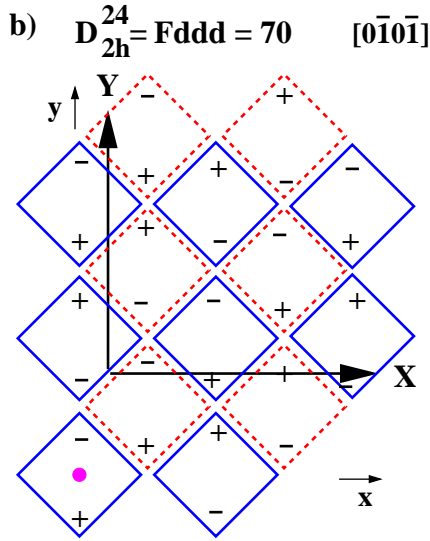
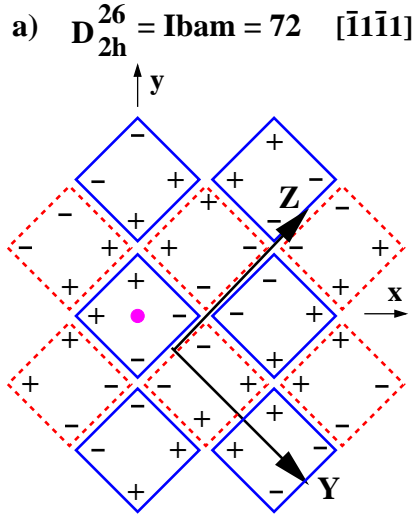


FIG. 12: (Color online) As Fig. 8 for the star of \mathbf{P} (variables change sign under $z \rightarrow z + 1$). x , y , and z are the tetragonal axes and X , Y , and Z are axes of the distorted structure. The new origins are in the $z = 3/4$ plane. The new out-of-plane lattice vector has magnitude 2 and is along z . The actual structures may involve an incommensurate wave vector near the star of \mathbf{P} .

A. The star of \mathbf{X}

1. θ structures

Using the symmetry operations of Table V we find that the free energy of the θ structures for the star of \mathbf{X} assumes the form

$$F(\theta) = c_\theta a^2 \lambda \sum_{k=1}^2 \sum_{\alpha=a}^b \left[(2\theta_{k\alpha}^2 + \epsilon_{xx})^2 + (2\theta_{k\alpha}^2 + \epsilon_{yy})^2 \right] + \frac{1}{2} a \sum_{k=1}^2 (\theta_{ka}^2 + \theta_{kb}^2)$$

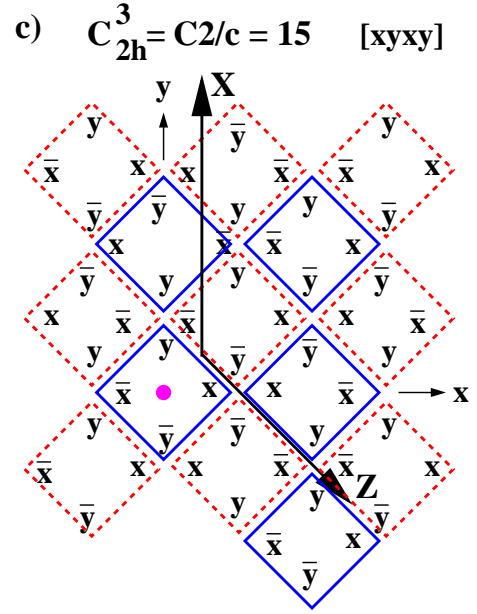


FIG. 13: (Color online) Continuation of Fig. 12. The new origin is in the $z = 1/4$ plane. The new out-of-plane lattice vector has magnitude 2 and is along z .

TABLE V: As Table I for the stars of \mathbf{X} and \mathbf{P} , except that this table is for the variables of RP327 systems. Note that $z = 0$ (about which m_z is taken) is midway between layers a and b . T is the translation $(1/2, 1/2, 1/2)$.

	\mathcal{R}_4	m_d	m_z	T
$\theta_{1,a}$	$\theta_{1,a}$	$-\theta_{1,a}$	$\theta_{1,b}$	$\theta_{2,a}$
$\theta_{1,b}$	$\theta_{1,b}$	$-\theta_{1,b}$	$\theta_{1,a}$	$\theta_{2,b}$
$\theta_{2,a}$	$-\theta_{2,a}$	$-\theta_{2,a}$	$\xi\theta_{2,b}$	$\xi\theta_{1,a}$
$\theta_{2,b}$	$-\theta_{2,b}$	$-\theta_{2,b}$	$\xi\theta_{2,a}$	$\xi\theta_{1,b}$
$\phi_{x,1}$	$\phi_{y,1}$	$\phi_{y,1}$	$\phi_{x,1}$	$\phi_{x,2}$
$\phi_{y,1}$	$-\phi_{x,1}$	$\phi_{x,1}$	$\phi_{y,1}$	$\phi_{y,2}$
$\phi_{x,2}$	$-\phi_{y,2}$	$\phi_{y,2}$	$\xi\phi_{x,2}$	$\xi\phi_{x,1}$
$\phi_{y,2}$	$\phi_{x,2}$	$\phi_{x,2}$	$\xi\phi_{y,2}$	$\xi\phi_{y,1}$

$$+b [\theta_{1a}\theta_{1b} + \theta_{2a}\theta_{2b}] + F_4 + F_{2\epsilon} . \quad (47)$$

For large λ , the minima of this free energy as $(a - |b|)$ passes through zero occur for

$$\begin{aligned} \epsilon_{xx} &= \epsilon_{yy} = -2\theta_{1a}^2 = -2\theta_{1b}^2 \\ &= -2\theta_{2a}^2 = -2\theta_{2b}^2 \\ \theta_{1a} &= -\frac{b}{|b|}\theta_{1b} , \quad \theta_{2a} = -\frac{b}{|b|}\theta_{2b} . \end{aligned} \quad (48)$$

Thus, as shown in Fig. 15, we have two possible distorted structures, depending on the sign of b :

$$\theta_{1,a} = -\theta_{1,b} = \xi\theta_{2,a} = -\xi\theta_{2,b} , \quad b > 0 \quad (49)$$

$$\theta_{1,a} = \theta_{1,b} = \xi\theta_{2,a} = \xi\theta_{2,b} , \quad b < 0 , \quad (50)$$

where $\xi = \pm 1$. The fact that ξ can have either sign indicates the decoupling of even and odd numbered sub-

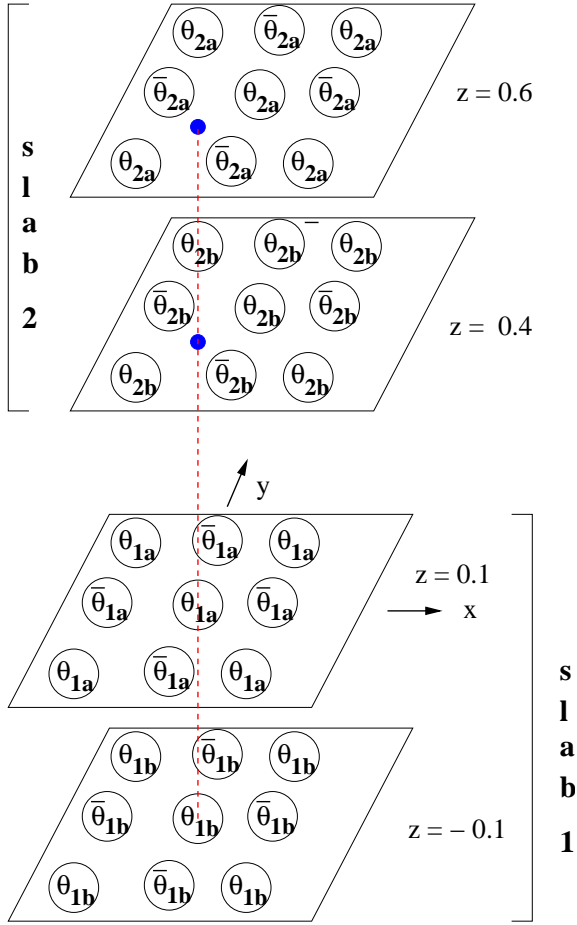


FIG. 14: (Color online) Values of the rotation (θ) variables in different z -planes for the most general such distortion of RP327's for the stars of \mathbf{X} and \mathbf{P} . The (red) dashed line is the axis about which the fourfold rotation \mathcal{R}_4 is taken and the (blue) dots show the points $x = y = 0$ in the $z = 0.4$ and $z = 0.6$ planes. Under \mathcal{R}_4 an octahedron in slab #1 is taken either into itself or into an equivalent octahedron. Under \mathcal{R}_4 an octahedron in slab #2 is taken into another whose rotation angle is of opposite sign. For the star of \mathbf{X} , $\theta_{n+2,x} = \theta_{n,x}$ and for the star of \mathbf{P} , $\theta_{n+2,x} = -\theta_{n,x}$.

lattices which we mentioned in connection with the analogous RP214 θ structures.

We now determine the space groups corresponding to these two modes. In the mode of Eq. (50) the two layers can be coalesced continuously into a single layer. So this structure has the same symmetry as the Cmca θ -structure resulting from the star of \mathbf{X} and is obtained by replacing each layer by a bilayer with in phase rotations. See Fig. 7a. The mode of Eq. (49) is shown in Fig. 16a. We have to discuss the way we depict bilayer systems in our figures. Within each square (which represents the equatorial oxygen of an octahedron) the symbols closer to the corners of the square apply to the upper layer of the bilayer and the symbols closer to the center apply to the lower layer of the bilayer. This convention does not

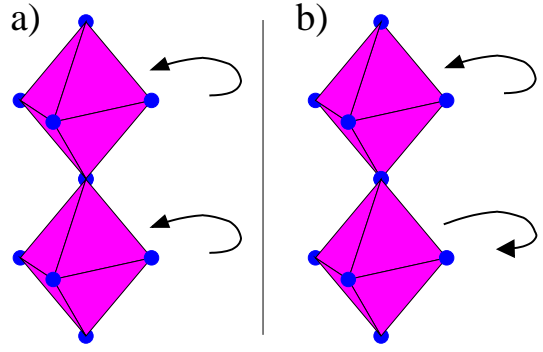


FIG. 15: (Color online) The two θ modes for a bilayer. Left: the two layers (a and b) rotate in phase as in Eq. (50). Right: the two layers rotate out of phase as in Eq. (49). The out of phase rotation increases the energy by twisting the oxygen orbitals but this is compensated by reducing the Coulomb interactions between octahedra. First principles calculations[30] indicate that these modes differ only slightly in energy.

cause undue difficulty in visualizing the effect of rotations about an axis perpendicular to the plane of the paper. However, operations such as reflection through the plane of the paper or inversion relative to the center of the octahedron introduce visual complications because these operation interchange inner and outer symbols. Experience indicates that for these operations one should use the results of Fig. 17, supplemented, if need be, by a translation. Operations such as $\mathcal{O} = (X, \bar{Y}, \bar{Z})$ which involve taking Z into $-Z$ are best expressed as $\mathcal{O} = \mathcal{I}(\bar{X}, Y, Z)$ or $\mathcal{O} = m_z(X, \bar{Y}, Z)$. The mirrors perpendicular to the page do not cause any confusion because for them outer symbols are taken into outer symbols, thus avoiding visual complications. We now return to the discussion of the mode of Eq. (49) in Fig. 16a. Using, if need be, the results of Fig. 17, one sees that this structure has generators $(X \pm 1/2, Y + 1/2, Z)$, $(X, Y, Z + 1)$, $(\bar{X}, \bar{Y}, \bar{Z})$, $(X + 1/2, \bar{Y}, \bar{Z} + 1/2)$, and $(\bar{X} + 1/2, \bar{Y}, Z)$, which therefore is Ccca (D_{2h}^{22}) #68 coming from irrep \mathbf{X}_1^- .

2. ϕ structures

Now we analyze the free energy for ϕ distortions at the star of \mathbf{X} . Here the effect of m_z has the opposite sign from the RP214 case. But since all terms are of even order, the symmetry of the free energy is the same as for RP214. So

$$\begin{aligned}
 F = & c_\theta a^2 \lambda \sum_{k=1}^2 \left[(2\phi_{xk}^2 + \epsilon_{xx})^2 + (2\phi_{yk}^2 + \epsilon_{yy})^2 \right] \\
 & + c_\phi a^2 \lambda \sum_{k=1}^2 (2\phi_{xk}\phi_{yk} + \epsilon_{xy})^2 \\
 & + [(\alpha - \beta)/2] [(\phi_{x,1} - \phi_{y,2})^2 + (\phi_{x,2} - \phi_{y,1})^2] \\
 & + [(\alpha + \beta)/2] [(\phi_{x,1} + \phi_{y,2})^2 + (\phi_{x,2} + \phi_{y,1})^2] \quad (51)
 \end{aligned}$$

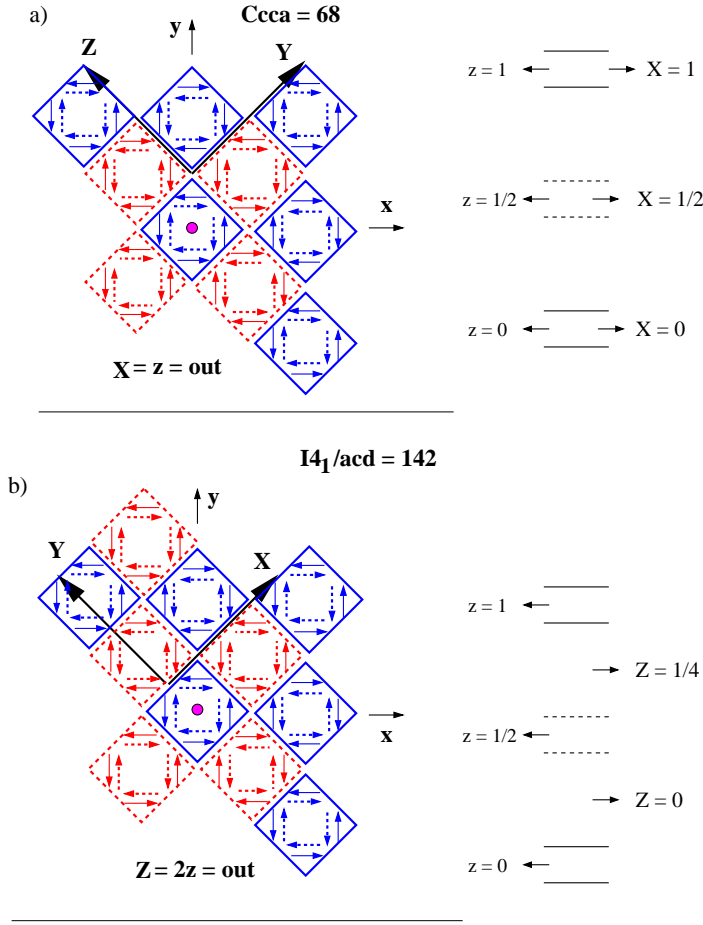


FIG. 16: (Color online) As Fig. 7. The θ -modes with $\theta_{n,a} = -\theta_{n,b}$. The full (dashed) squares are equatorial sections of the bilayer centered at $z = 0$ ($z = 1/2$). The outer full (inner dashed) arrows are the displacements of the equatorial oxygens in the equatorial plane in the upper (lower) layer of the bilayer. In the upper (lower) panel the arrows are unchanged (reversed) under $z \rightarrow z + 1$. The new origin is at $z = 0$ in the upper panel and at $z = 1/4$ in the lower panel. At right we show the z -coordinates of the full and dashed layers.

where $\phi_{\alpha,n}$ is the value of ϕ_{α} for the top layer of the n th ($n = 1, 2$) slab.

The analysis parallels that for RP214 systems. Here we characterize the structures by the values of $\phi_{n,\alpha}$ in the *top* layer of each bilayer. From the first line we conclude that $\phi_{x1}^2 = \phi_{x2}^2$ and $\phi_{y1}^2 = \phi_{y2}^2$. There are two cases: the first is if $\alpha - \beta$ is critical and the second is if $\alpha + \beta$ is critical. In the first case $\phi_{x1} = -\phi_{y2}$ and $\phi_{x2} = -\phi_{y1}$. In the second case $\phi_{x2} = \phi_{y1}$ and $\phi_{x1} = \phi_{y2}$. Then for the first case the possible ordering vectors are proportional to $\Phi = [11\bar{1}\bar{1}]$ or $[\bar{1}\bar{1}11]$. These are equivalent structures and we take the second one as the representative for this case. For the second case the possible ordering vectors are proportional to $\Phi = [1111]$ and $[\bar{1}\bar{1}\bar{1}\bar{1}]$. These are equivalent structures and we take $[\bar{1}\bar{1}\bar{1}\bar{1}]$ as the representative for this case. Fig. 18 shows these representatives.

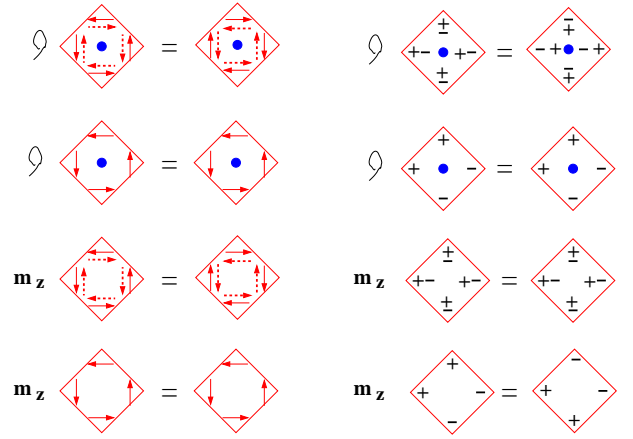


FIG. 17: (Color online) The effect of operations which take Z into $-Z$. Here the distortion of a bilayer is represented by two sets of symbols within the square representing the equatorial oxygens. The outer set of symbols applies to the upper layer of the bilayer and the inner set to the lower layer of the bilayer. Inversion (\mathcal{I}) is taken with respect to the (blue) filled circle as the origin, which for bilayers is in the plane midway between the upper and lower layer. m_z is a mirror operation with respect to the plane perpendicular to the tetragonal z -axis which passes through the origin.

Finally, we identify the space groups of the structures of Fig. 18. Note that $\alpha + \beta$ critical corresponds to irrep X_4^- and $\alpha - \beta$ critical corresponds to irrep X_3^- in the notation Ref. 19. The generators of $[\bar{1}\bar{1}\bar{1}\bar{1}]$ are $(X \pm 1/2, Y + 1/2, Z)$, $(X, Y, Z + 1)$, $(\bar{X} + 1/2, \bar{Y}, Z)$, (X, \bar{Y}, \bar{Z}) , and $(\bar{X}, \bar{Y}, \bar{Z})$ and those of $[1111]$ are $(X \pm 1/2, Y + 1/2, Z)$, $(X, Y, Z + 1)$, $(\bar{X}, \bar{Y}, \bar{Z})$, $(\bar{X}, \bar{Y}, Z + 1/2)$, and (X, \bar{Y}, \bar{Z}) . From these generators we identify the space groups as indicated in Fig. 18.

B. The star of N

Again the analysis parallels that for RP214. Now the analog of Table IV is Table VI.

TABLE VI: As Table I, but for the RP327 variables of the star of $\mathbf{N} \equiv (1/2, 0, 1/2)$ (shown in Fig. 9). $T \equiv (1/2, 1/2, 1/2)$, $T_x \equiv (1, 0, 0)$, and $T_y \equiv (0, 1, 0)$. All variables are odd under $\mathbf{T} \equiv (0, 0, 1)$.

	\mathcal{R}_4	m_d	m_z	T	T_x	T_y
$\phi_{x,1}$	$\phi_{y,1}$	$\phi_{y,1}$	$\phi_{x,1}$	$\phi_{x,2}$	$-\phi_{x,1}$	$\phi_{x,1}$
$\phi_{y,1}$	$-\phi_{x,1}$	$\phi_{x,1}$	$\phi_{y,1}$	$\phi_{y,2}$	$\phi_{x,1}$	$-\phi_{y,1}$
$\phi_{x,2}$	$\phi_{y,2}$	$\phi_{y,2}$	$-\phi_{x,2}$	$-\phi_{x,1}$	$-\phi_{x,2}$	$\phi_{x,2}$
$\phi_{y,2}$	$\phi_{x,2}$	$\phi_{x,2}$	$-\phi_{y,2}$	$-\phi_{y,1}$	$\phi_{y,2}$	$-\phi_{y,2}$

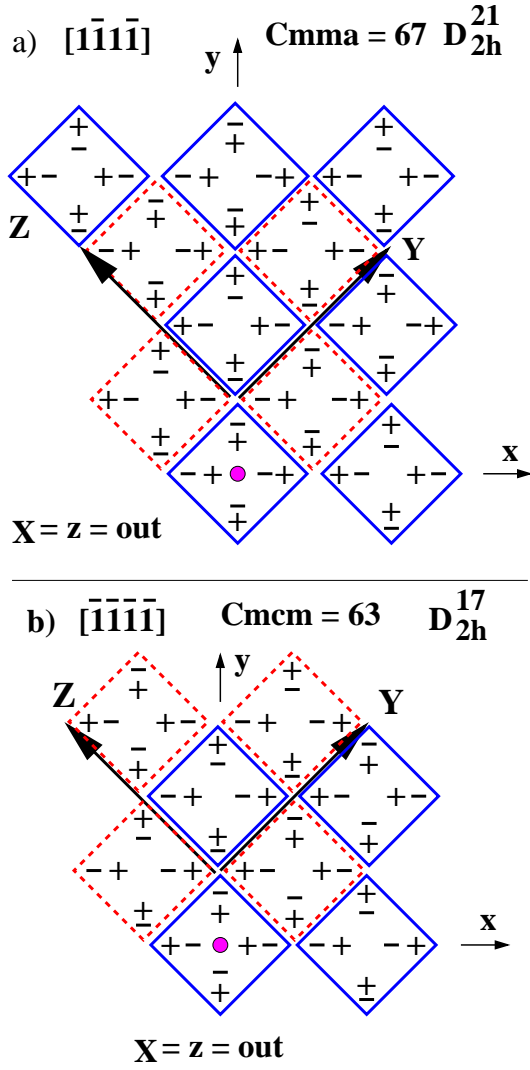


FIG. 18: (Color online) As Fig. 6 but for the star of \mathbf{X} for RP327 (with invariance under $z \rightarrow z + 1$). x , y , and z are the tetragonal axes and X , Y , and Z are the conventional lattice vectors after distortion. The filled magenta circle is the tetragonal origin. The outer + or - sign gives the sign of the z -component of displacement of the upper layer of the bilayer and the inner + or - sign gives the sign of the z -component of displacement of the lower layer of the bilayer. $\Psi = [\bar{1}\bar{1}\bar{1}\bar{1}]$ for a) and $[\bar{1}\bar{1}\bar{1}\bar{1}]$ for b). The new origin is in the $z = 0$ plane. The third new axis vector is $[001]$ in terms of the original tetragonal coordinates.

The free energy for the star of \mathbf{N} is then

$$F = c_\theta a^2 \lambda \sum_{k=1}^2 \left[(2\phi_{xk}^2 + \epsilon_{xx})^2 + (2\phi_{yk}^2 + \epsilon_{yy})^2 \right] + \frac{\alpha}{2} [\phi_{x,1}^2 + \phi_{y,1}^2 + \phi_{x,2}^2 + \phi_{y,2}^2] + F_{2\epsilon} + F_4 \quad (52)$$

This free energy is the same as for RP214, so the structures for RP327 will be related to those of RP214. In Fig. 19 we show the structures in which the ϕ 's for the

upper layer are identical to those of the single layer in Fig. 10. Note that of all the generators of Fig. 10, only inversion $(\bar{X}, \bar{Y}, \bar{Z})$ connects the $z = n$ layers to the $z = n + 1/2$ layers. Also note that according to Fig. 17 inversion for $n = 2$ systems introduces an extra minus sign compared to the $n = 1$ case. This fact suggests that by appropriately placing the new origins (as we have done in Fig. 19) one can pass from RP214 to RP327, otherwise keeping the structure (and the space group) unchanged. We thereby determine the generators to be the same as for the analogous structures in Fig. 10: for $[\bar{x}y\bar{x}y]$ the generators are $(X + 1, Y, Z)$, $(X, Y + 1, Z)$, $(X, Y, Z + 1)$, and $(\bar{X}, \bar{Y}, \bar{Z})$, which is C_i^1 ($P\bar{1} = \# 2$). For both $[010\bar{1}]$ and $[\bar{1}\bar{1}\bar{1}\bar{1}]$, the generators are $(X, Y, Z + 1)$, $(X + 1/2, Y + 1/2, Z)$, $(X + 1/2, Y - 1/2, Z)$, $(\bar{X}, \bar{Y}, \bar{Z})$, and (\bar{X}, Y, \bar{Z}) which is C_{2h}^3 ($C2/m = \#12$). Although these two structures belong to the same space group, they are different because their unit cells are different (see Fig. 10).

C. The star of \mathbf{P}

1. θ structures

The situation for θ -structures at the star of \mathbf{P} is similar to that at the star of \mathbf{X} except that the displacements change sign under $z \rightarrow z + 1$. The structures with $\theta_{n,a} = \theta_{n,b}$ have the same symmetry as that shown in Fig. 7b: however, each single layer is replaced by a bilayer in which $\theta_{n,a} = \theta_{n,b}$. So the space group is again $I4_1/acd = \#142$ (D_{4h}^{20}). The structure with $\theta_{n,a} = -\theta_{n,b}$ and which changes sign under $z \rightarrow z + 1$ is illustrated in Fig. 16b. This structure is generated by $(X - 1/2, Y + 1/2, Z + 1/2)$, $(X + 1/2, Y - 1/2, Z + 1/2)$, $(X + 1/2, Y + 1/2, Z - 1/2)$, $(\bar{X}, \bar{Y}, \bar{Z})$, $(X, \bar{Y}, \bar{Z} + 1/2)$, and $(\bar{Y} + 1/4, X + 3/4, Z + 1/4)$ and is therefore $I4_1/acd = \#142$ (D_{4h}^{20}) coming from irrep P_2 . In identifying the generators we used Fig. 17.

2. ϕ structures

To identify the space groups of the structures shown in Fig. 20 recall the discussion just below Eq. (52). By shifting the new origin, we identify the generators as: (X, Y, \bar{Z}) , $[44]$ $(X, \bar{Y}, \bar{Z} + 1/2)$, $(\bar{X}, \bar{Y}, \bar{Z})$, $(X - 1/2, Y + 1/2, Z + 1/2)$, $(X + 1/2, Y - 1/2, Z + 1/2)$, and $(X + 1/2, Y + 1/2, Z - 1/2)$ for a), $(\bar{X} + 1/4, \bar{Y} + 1/4, Z)$, $(X, \bar{Y} + 1/4, \bar{Z} + 1/4)$, $(\bar{X}, \bar{Y}, \bar{Z})$, $(X - 1/2, Y + 1/2, Z + 1/2)$, $(X + 1/2, Y - 1/2, Z + 1/2)$, and $(X + 1/2, Y + 1/2, Z - 1/2)$ for b), and (\bar{X}, Y, \bar{Z}) , $(\bar{X}, \bar{Y}, \bar{Z})$, $(X + 1, Y, Z)$, $(X, Y + 1, Z)$, and $(X, Y, Z + 1)$ for c). These lead to the space groups listed in the figure. Because of the Lifshitz instability the wave vector is an incommensurate one close to \mathbf{P} , as is discussed in Sec. III.2.

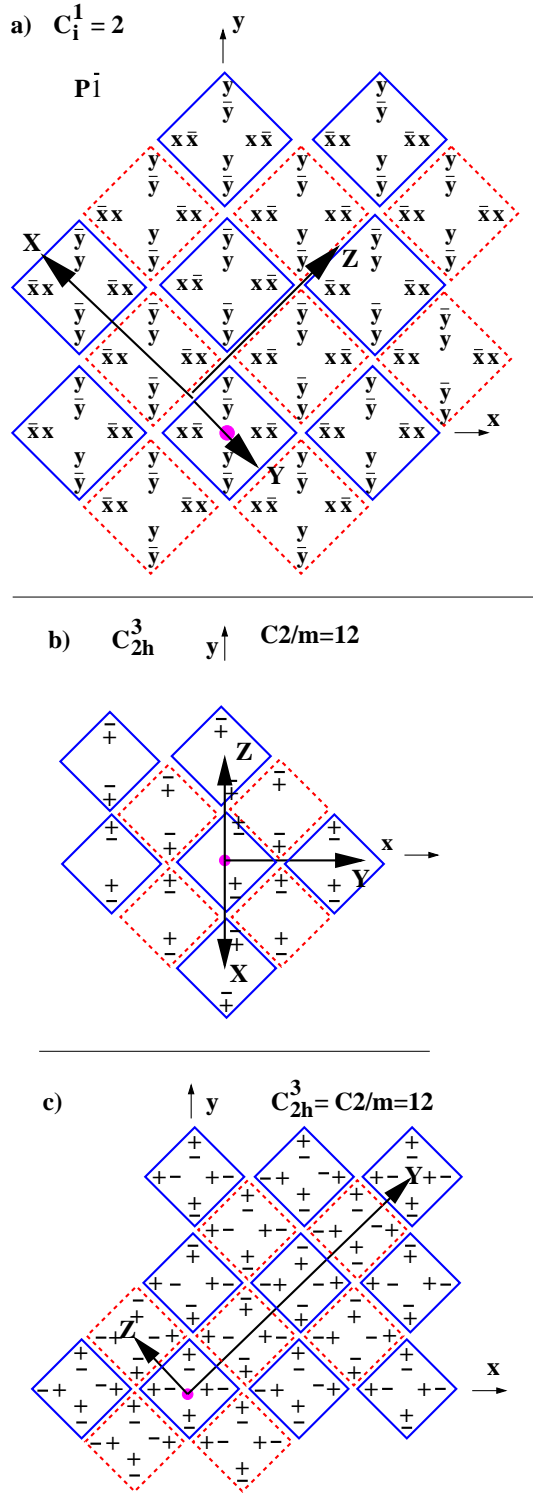


FIG. 19: (Color online) As Fig. 18 but for the star of \mathbf{N} (with sign change under $z \rightarrow z + 1$) for a) $[\bar{x}y\bar{x}y]$, b) $[0\bar{1}0\bar{1}]$, and c) $[\bar{1}\bar{1}\bar{1}\bar{1}]$. The new origins are at $z = 1/4$ for a) and at $z = 1/2$ for b) and c).

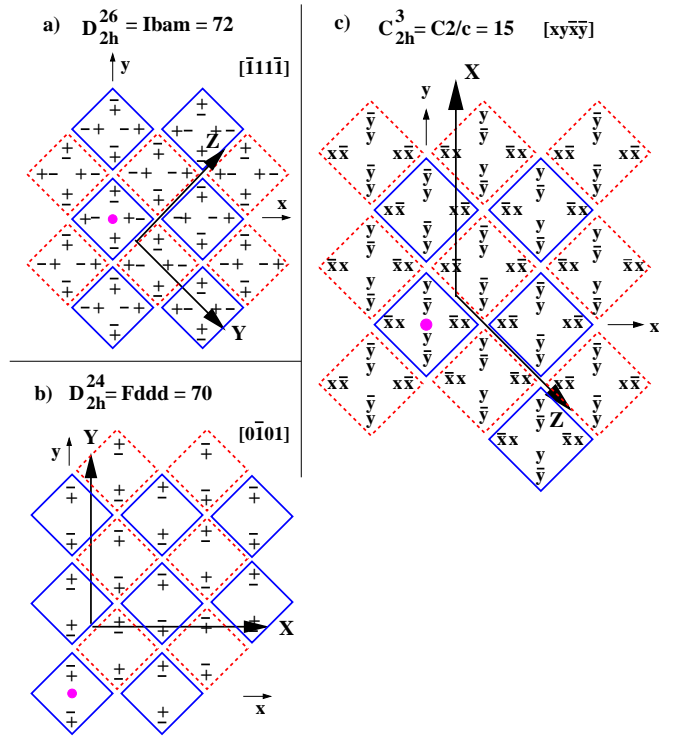


FIG. 20: (Color online) As Fig. 18 but for the star of \mathbf{P} (with sign change under $z \rightarrow z + 1$) for a) $[\bar{1}\bar{1}\bar{1}\bar{1}]$, b) $[0\bar{1}0\bar{1}]$, and c) $[xy\bar{x}y]$. The new origins are at $z = 3/4$ in a) and in b) and at $z = 1/4$ in c). The new out-of-plane axes are $(0, 0, 2)_t$.

V. RP SYSTEMS WITH $n > 2$

Now we are in a position to analyze the situation of RP systems with $n > 2$. For the θ -structures the important issue is whether the eigenvalue $\lambda(M_z)$ which gives the symmetry of the stacking sequence is $+1$ or -1 . For the ϕ -structures the important issue is, as stated in Ref. 20, whether n , the number of layers per substructure, is even or odd.

A. θ -structures

We first consider θ -structures. The θ -structures associated with the star of either \mathbf{X} or of \mathbf{P} are governed by the free energy

$$F = \sum_{m=1}^2 \sum_{k=1}^n \left[(2\theta_{mk}^2 - \epsilon_{xx})^2 + (2\theta_{mk}^2 - \epsilon_{yy})^2 \right] + \sum_{m=1}^2 \sum_{k,l=1}^n A_{k,l} \theta_{m,k} \theta_{m,l} + V, \quad (53)$$

where V contains interaction terms (of order λ^0) between the two different slabs. Note that quadratic terms like $\theta_{1,\alpha} \theta_{2,\beta}$ are excluded because they are not invariant un-

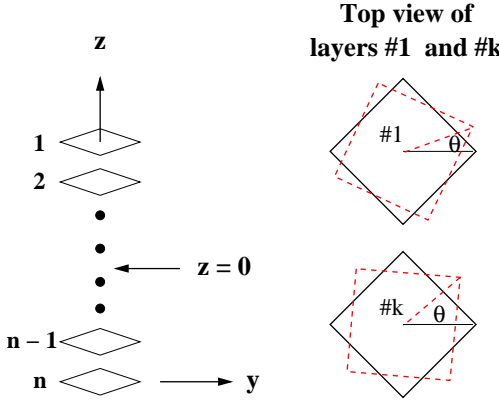


FIG. 21: (Color online) The θ -structures for one of the n -layer slabs. Left: The cross section of the n -layer slab showing the (x, y, z) coordinate system used to discuss the symmetry of the θ -structures. Right: Top view showing that the structure (red dashed cross section) is characterized by giving the value of the rotation θ for each of the n layers.

der \mathcal{R}_4 , as one sees from Table V or Fig. 14. The ordering vector of the first n -layer slab in the unit cell is

$$\Phi_1 = [\theta_{1,1}, \theta_{1,2}, \theta_{1,3} \dots \theta_{1,n}] . \quad (54)$$

Note that Φ is proportional to the eigenvector of the matrix \mathbf{A} which has the minimal eigenvalue (so that it is the one which first becomes critical as the temperature is lowered). The matrix \mathbf{A} is invariant under the mirror operation M_z which interchanges layers k and $n+1-k$, so that $\theta_k \leftrightarrow \theta_{n+1-k}$. Therefore we know only that the eigenvector is either even or odd (*i. e.* the eigenvalue of M_z , $\lambda(M_z)$, is either $+1$ or -1 , respectively), depending on the details of the interactions in the system. For instance, for $n=1$ $\Phi_1 = [1]$ and is even under M_z . For $n=2$ the critical eigenvector is either $[11]$ (which is even under M_z) or $[1\bar{1}]$ (which is odd under M_z). For $n=3$ the critical eigenvector is either $[10\bar{1}]$ (which is odd under M_z) or $[\alpha\beta\alpha]$, where α and β depend on the interactions within the 3-layer subsystem and this eigenvector is even under M_z . On the basis of symmetry we can definitely *not* posit any specific form for the eigenvector (for $n > 2$), as is done in Table XIII of Ref. 20. In all these examples the ordering vector for the second n -layer subsystem obeys $\Phi_2 = \pm\Phi_1$, where the indeterminacy in sign reflects the by now familiar frustration of θ structures.

For $n > 2$ the state we call I, given by the critical eigenvector of \mathbf{A} , will develop at the structural phase transition at a critical temperature we denote T_I . For this state θ_k^2 will not be independent of k unless there is an unusual accidental degeneracy and therefore its free energy will be of the form

$$F_I = \frac{1}{2}(T - T_I)Q_I^2 + \alpha\lambda Q_I^4 . \quad (55)$$

The quartic term must be of order λ because θ_k^2 is *not* independent of k . This state competes with state II which

satisfies (for all k and l)

$$2\theta_{kl}^2 = -\epsilon_{xx} = -\epsilon_{yy} . \quad (56)$$

State I becomes critical at a temperature T_I which is higher than that, T_{II} , at which state II becomes critical. The free energy of state II can be written as

$$F_{II} = \frac{1}{2}(T - T_{II})Q_{II}^2 + \beta Q_{II}^4 . \quad (57)$$

Minimization with respect to the order parameters yields

$$F_I = -\frac{1}{2} \frac{(T - T_I)^2}{\alpha\lambda} \quad T < T_I , \quad F_I = 0 , \quad T > T_I$$

$$F_{II} = -\frac{1}{2} \frac{(T - T_{II})^2}{\beta} \quad T < T_{II} , \quad F_{II} = 0 , \quad T > T_{II}$$

and these are plotted versus T in Fig. 22. One sees that for $n > 2$ we have a more complicated phase diagram than for $n=1$ or 2 . When λ is large, for a small range of temperature phase I is stable, but at lower T we arrive at phase II. For $n > 3$ it is possible to have more than one phase transition before ultimately reaching phase II.

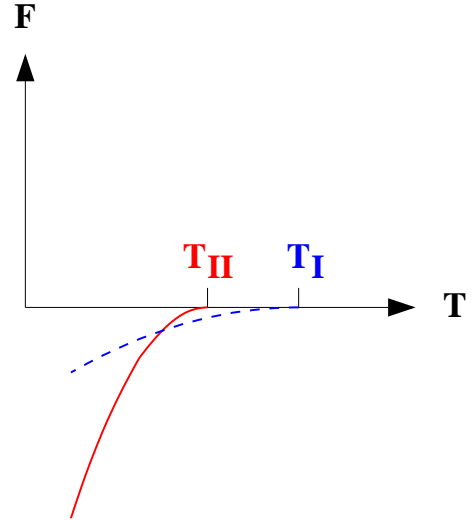


FIG. 22: (Color online) The free energies of phase I (dashed line) and phase II (full line), as given by Eq. (58). These curves are drawn for $\alpha\lambda/\beta = 9$.

The possible θ -structures of phase I depend on the wave vector (\mathbf{X} or \mathbf{P}) and whether the interactions within the system select $\lambda(M_z) = +1$ or -1 . First consider the star of \mathbf{X} , for which $\theta_{m+2,k} = \theta_{m,k}$. If $\lambda(M_z) = +1$ (as in Fig. 7a), then, irrespective of the value of the number of layers per subsystem, we will have a structure similar to that of Fig. 7a (in which each layer of Fig. 7 is replaced by an n -layer slab) with space group $\text{Cmca}=\#64$. If interactions select, $\lambda(M_z) = -1$ (this is only possible for $n > 1$), then we have a structure of space group $\text{Ccca}=\#68$, similar to that shown in Fig. 16a. Next consider the star of \mathbf{P} , for which $\theta_{m+2,k} = -\theta_{m,k}$. If

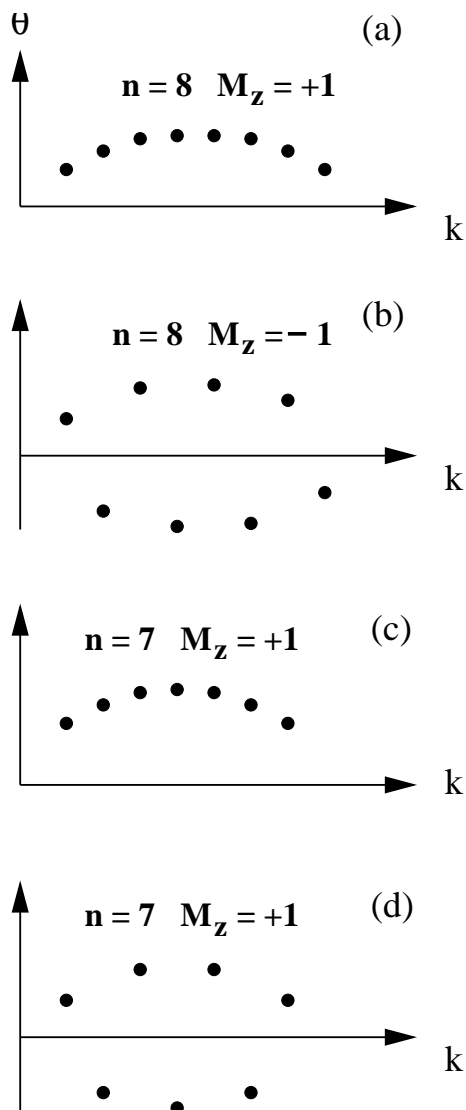


FIG. 23: Typical variation of θ as a function of the layer index, k , for dominant nearest neighbor interlayer interaction, $A_{k,k+1} \equiv w$. For case (a), n is even and $w < 0$, so that $\lambda(M_z) = +1$. For case (b), n is even and $w > 0$, so that $\lambda(M_z) = -1$. For cases (c) and (d) n is odd. For case (c) $w < 0$ and for case (d) $w > 0$. In both cases $\lambda(M_z) = +1$. To obtain $\lambda(M_z) = -1$ for n odd requires further neighbor interlayer interactions.

$\lambda(M_z) = +1$ (as in Fig. 7b), then, irrespective of the value of the number of layers per subsystem, we will have a structure similar to that of Fig. 7b with space group $I4_1/acd=\#142$. If interactions select $\lambda(M_z) = -1$ (this is only possible for $n > 1$), then we have a structure of space group $I4_1/acd=\#142$, similar to that shown in Fig. 16b.

The above remarks relied only on symmetry. However, now we consider the likely form of the interaction matrix $A_{k,l}$ in Eq. (53) which determines θ as a function of the layer index k . If the dominant intraslab interactions are

TABLE VII: Summary of results for commensurate structures for RP n layer systems. \vec{Q} denotes the wave vector, Var labels the angular variable, and λ is the eigenvalue of the mirror operation within the n -layer substructure, as discussed below Eq. (54). In the last column we indicate whether the transition is allowed to be continuous (Y) or not (N) or whether there is a Lifshitz instability (L). See Ref. 19. The results in this table can be compared to the results for the X point given in Table XIII of Ref. 20. Our analysis only allows structures #2, 5, 9, and 12 of that reference.

\vec{Q}	Var	λ	Space group(s)	n	See Fig.	Y,N,L
X	θ	-1	#68 (D_{2h}^{22}) Ccca	$n > 1^*$	14a	Y
X	θ	+1	#64 (D_{2h}^{18}) Cmca	$n \geq 1$	7a	Y
P	θ	+1	#142 (D_{4h}^{20}) $I4_1/acd$	$n \geq 1$	7b	Y
P	θ	-1	#142 (D_{4h}^{20}) $I4_1/acd$	$n > 1^*$	14b	Y
X	ϕ	-1	#64 (D_{2h}^{18}) Cmca	odd	8a	Y
			#66 (D_{2h}^{20}) Cccm	odd	8b	Y
X	ϕ	+1	#63 (D_{2h}^{17}) Cmcm	even	16c	Y
			#67 (D_{2h}^{21}) Cmma	even	16a	Y
N	ϕ	-1	#12 (C_{2h}^3) C2/m	odd	10b	N
			#12 (C_{2h}^3) C2/m	odd	10c	N
			#2 (C_i^1) $P\bar{1}$	odd	10a	N
N	ϕ	+1	#12 (C_{2h}^3) C2/m	even	17b	N
			#12 (C_{2h}^3) C2/m	even	17c	N
			#2 (C_i^1) $P\bar{1}$	even	17a	N
P	ϕ	-1	#72 (D_{2h}^{26}) Ibam	odd	11a	L
			#70 (D_{2h}^{24}) Fddd	odd	11b	L
			#15 (C_{2h}^3) C2/c	odd	11c	L
P	ϕ	+1	#72 (D_{2h}^{26}) Ibam	even	18a	L
			#70 (D_{2h}^{24}) Fddd	even	18b	L
			#15 (C_{2h}^3) C2/c	even	18c	L

* If the dominant interlayer interactions are those between adjacent layers, then, as discussed in the text, n must be even for this case to occur.

those between adjacent layers, then, as illustrated in Fig. 23, we obtain configurations analogous to ferromagnetic (panel a) or antiferromagnetic (panel b) spin structures. Thus, with nearest neighbor interlayer interactions, if n , the number of layers per slab is even, we can have either sign of $\lambda(M_z)$. If n is odd, then this special ansatz of nearest neighbor interlayer interactions can only give $\lambda(M_z) = +1$. If, experimentally, the case $\lambda(M_z) = -1$ is observed for odd n , one could conclude the existence of significant longer range interlayer interactions. (Such a situation is obviously possible in the presence of Coulomb interactions.)

Our results are summarized in Table VII. Note that for the θ structures the controlling variable is not the number of layers n , but $\lambda(M_z)$. It is interesting to note that for **N** and **P**, the ϕ -structures for even and odd $\lambda(M_z)$ are very similar. Apart from the fact that their substructures are different, they only differ in the location of the center of inversion symmetry.

VI. DISCUSSION AND CONCLUSION

We did not deal with the positions of the ions at the center of the octahedra or those between the layers of octahedra. Here we are only concerned with such ionic positions as they are modified by the orientational structural transition. Each such ion sits in a stable potential well. The question is whether or not for systems without any accidental degeneracy there is a bifurcation so that additional space groups could be allowed when the positions of these “inessential” ions are taken into account. The stable potential well can be distorted and the placement of its minimum will be modified by the octahedral reorientation. But a single minimum of a stable potential well can not be continuously deformed into a double well without assuming an accidental vanishing of the fourth order term in the local potential. Similar arguments show that the perturbative effect of the center of mass coordinates of the nearly rigid octahedra do not produce anomalous effects. Of course, parameters of Wyckoff orbits which are not fixed by symmetry will be perturbatively modified at the structural phase transition. Similarly, the elastic strain tensor will be perturbatively modified consistent with the symmetry of the resulting phase at the transition.

Experimentally, it is striking that the structures observed as distortions from the tetragonal phase are in our much shorter list. For instance, in the data cited on p 313 and ff of Ref. 20 five systems with ϕ tilts are shown which go into either Cmca (64) or P4₂/ncm (138), except for Rb₂CdCl₄ whose structure is uncertain: either Cmca or Fccm (which is on neither our list nor that of Ref. 17 because it involves two irreps). Systems (other than Rb₂CdCl₄ subsequently discussed in Ref. 20) in Table III of Ref. 17 likewise go into either Cmca or P4₂/ncm.

To summarize: we have analyzed the possible structural transitions of the so-called Ruddlesden-Popper perovskite structure (such as K₂MnF₄ or Ca₃Mn₂O₇, etc.) using a variant of Landau theory in which the constraint of rigid oxygen octahedra is implemented and our results are compared to the well-known results of Refs. 17 and 20. A check on the accuracy of our treatment of symmetry is that our list of allowed structures (for K₂MgF₄) which can be reached via a single structural phase transition is a *subset* of the list of Ref. 17. We find that the rigid octahedral constraint eliminates all the structures in Table I of Ref. 17 for which the octahedral tilting transitions are discontinuous. It is also appealing that structures which are allowed by symmetry but which involve undistorted sublattices are eliminated by the octahedral constraint. The results for the K₂MgF₄ structure are summarized in Tables II and III, where one sees that our list of possible structures is a much reduced subset of Ref. 17. For these systems, our analysis allows (see Tables II and III) only 13 of the 41 structures listed in Ref. 17 and of these only nine are commensurate structures. A summary of our results for commensurate structures for A_{n+1}B_nC_{3n+1} is given in Table VII.

ACKNOWLEDGEMENTS: I am grateful to T. Yildirim for performing the first principles calculations. I thank J. M. Perez-Mato, C. J. Fennie, B. Campbell, and H. T. Stokes for helpful discussions.

Appendix A: Minimization to order λ^{-1}

Here we show that corrections of order $1/\lambda$ to the minimization of the free energy do not qualitatively affect our conclusions. We consider the free energy

$$\begin{aligned}
 F = & c_{\theta} a^2 \lambda \left[\left(\frac{1}{2} \theta_1^2 + \epsilon_{xx} \right)^2 + \left(\frac{1}{2} \theta_2^2 + \epsilon_{xx} \right)^2 \right. \\
 & \left. + \left(\frac{1}{2} \theta_1^2 + \epsilon_{yy} \right)^2 + \left(\frac{1}{2} \theta_2^2 + \epsilon_{yy} \right)^2 \right] \\
 & - \frac{1}{2} |\gamma| [\theta_1^2 + \theta_2^2] + \frac{1}{2} \sum_{j,k} c_{j,k} \epsilon_j \epsilon_k \\
 & + \frac{1}{4} u [\theta_1^4 + \theta_2^4] + \frac{1}{2} v \theta_1^2 \theta_2^2 - d \epsilon_{xy} \theta_1 \theta_2 \\
 & + [b (\epsilon_{xx} + \epsilon_{yy}) + c c_{zz}] [\theta_1^2 + \theta_2^2] \quad (A1)
 \end{aligned}$$

where all the coefficients except λ are of order unity and the summation is in Voigt notation. We assume that nonlinear elastic terms (of higher than quadratic order) in ϵ can be neglected. We now set

$$\begin{aligned}
 \epsilon_{xx} &= -\frac{1}{4} [\theta_1^2 + \theta_2^2] + \xi_x \\
 \epsilon_{yy} &= -\frac{1}{4} [\theta_1^2 + \theta_2^2] + \xi_y \quad (A2)
 \end{aligned}$$

The terms involving λ become

$$F(\lambda) = \frac{1}{4} c_{\theta} a^2 \lambda (\theta_1^2 - \theta_2^2)^2 + 2 c_{\theta} a^2 \lambda [\xi_x^2 + \xi_y^2] \quad (A3)$$

Therefore the quartic terms in θ_k are of the form of Eq. (4) where v is surely negative for large λ . Accordingly, to all orders in $1/\lambda$ we may set

$$\theta_1^2 = \theta_2^2 \equiv \theta(\lambda) \quad (A4)$$

Also we see that the coefficients of terms linear in ϵ_{xx} and ϵ_{yy} are equal. So we may set $\xi_x = \xi_y \equiv \xi$. Then ξ is determined to leading order in $1/\lambda$ by

$$\begin{aligned}
 F = & 4 c_{\theta} a^2 \lambda \xi^2 - |\gamma| \theta^2 + U \theta^4 + \frac{1}{2} c_{33} \epsilon_{zz}^2 \\
 & + [(4b - x_{11}) \xi + 2 c c_{zz}] \theta^2 + \frac{1}{2} c_{44} \epsilon_{xy}^2 \\
 & - d \epsilon_{xy} \theta_1 \theta_2 \quad (A5)
 \end{aligned}$$

where

$$U = \frac{1}{2} (u + v) - 2b + \frac{1}{4} c_{11} \quad (A6)$$

Then, by minimizing F of Eq. (A5) with respect to ξ , we get $\xi \sim \lambda^{-1}$ or

$$\epsilon_{xx} = \epsilon_{yy} = -\frac{1}{2}\theta^2 + e\lambda^{-1}, \quad (\text{A7})$$

where e is of order λ^0 . This tells us that the octahedral mismatch (or distortion) is not zero, but is of order λ^{-1} . The corrections of order $1/\lambda$ to the elastic constants, do not, of course affect the symmetry of the structure.

-
- ¹ S. N. Ruddlesden and P. Popper, *Acta Cryst.* **11**, 54 (1958).
- ² J. D. Bednorz and K. A. Müller, *Z. Phys.* **B64**, 189 (1986).
- ³ Y. Tokura (Ed.), *Colossal Magnetoresistance Oxides*, Monograph in Condensed Matter Science, Gordon and Breach, London, 2000.
- ⁴ J. F. Mitchell, D. N. Argyriou, A. Burger, K. E. Grey, R. Osborn, and U. Welp, *J. Phys. Chem. B* **105**, 10732 (2001).
- ⁵ M. V. Lobanov, M. Greenblatt, El'ad N. Caspi, J. D. Jorgensen, D. V. Sheptyakov, B. H. Toby, C. E. Botez, and P. W. Stephens, *J. Phys.: Condens. Matter* **16**, 5339 (2004).
- ⁶ N. A. Benedek and C. J. Fennie, *Phys. Rev. Lett.* **106**, 107204 (2011).
- ⁷ A. B. Harris, *Phys. Rev. B*, in press.
- ⁸ *International Tables for Crystallography*, edited by Th. Hahn (Kluwer Academic, Dordrecht, 1995), Vol. A.
- ⁹ K. R. Poeppelmeier, M. E Leonowicz, J. C. Scanlon, J. M. Longo, and W. B. Yelon, *J. Solid State Chem.* **45**, 71 (1982).
- ¹⁰ M. E Leonowicz, K. R. Poeppelmeier, and J. M. Longo, *J. Solid State Chem.* **71**, 59 (1985).
- ¹¹ P. D. Battle, M. A Green, N. S. Laskey, J. E. Millburn, L. Murphy, M. J. Rosseinsky, S. P. Sullivan, and J. F. Vente, *Chem. Mater.* **9**, 552 (1997).
- ¹² P. D. Battle, M. A Green, J. Lago, J. E. Millburn, M. J. Rosseinsky, and J. F. Vente, *Chem. Mater.* **10**, 658 (1998).
- ¹³ I. D. Fawcett, J. E. Sunstrom IV, M. Greenblatt, M. Croft, and K. V. Ramanujachary, *Chem. Mater.* **10**, 3643 (1998).
- ¹⁴ A. M. Glazer, *Acta Cryst.* **B28**, 3384 (1972).
- ¹⁵ P. M. Woodward, *Acta Cryst.* **B53**, 32 (1997).
- ¹⁶ K. S. Aleksandrov, B. V. Beznosikov, and S. V. Misyul, *Phys. Status Solidi A* **104**, 529 (1987).
- ¹⁷ D. M. Hatch, H. T. Stokes, K. Aleksandrov, and S. V. Misyul, *Phys. Rev. B* **39** 9282 (1989).
- ¹⁸ ISODISTORT (accessible from the internet).
- ¹⁹ H. T. Stokes and D. M. Hatch, *Isotropy Subgroups of the 230 Crystallographic Space Groups* (World-Scientific, Singapore, 1988).
- ²⁰ K. S. Aleksandrov and J. Bartolomé, *J. Phys. Condens. Matter* **6**, 8219 (1994). K. S. Aleksandrov and J. Bartolomé, *Phase Transitions* **74**, 255 (2001). Our results do not seem to agree with these papers.
- ²¹ A shorter version of this paper (dealing only with RP214 systems and not including strain effects) is at arXiv:1012.5127.
- ²² A summary of relevant data for pseudocubic perovskites is given by J.-S. Zhou and J. B. Goodenough, *Phys. Rev. B* **77**, 131104 (2008).
- ²³ Lengths are in units of lattice constants a_i and wave vectors in units of $2\pi/a_i$.
- ²⁴ See Wikipedia under "Multicritical point."
- ²⁵ A. D. Bruce and A. Aharony, *Phys. Rev. B* **11**, 478 (1975).
- ²⁶ Since we focus on the displacements of ions, we denote the displacements as θ and ϕ_α rather than $a\theta/2$ and $a\phi_\alpha/2$, as we would if θ and ϕ_α were the angle variables. In addition, note that ϕ_x (ϕ_y) originates from a rotation of magnitude $\phi_x/2$ ($\phi_y/2$) about the y (x) axis.
- ²⁷ A criticism taken from a referee report of arXiv:1012.5127.
- ²⁸ J. M. Perez-Mato, M. Aroyo, A. Garcia, P. Blaha, K. Schwarz, J. Schwiefer, and K. Parlinski, *Phys. Rev. B* **70**, 214111 (2004).
- ²⁹ J. López-Perez and J. Íñiguez, arXiv:1101.2066v1.
- ³⁰ T. Yildirim, to be published.
- ³¹ See "Hooke's Law" in wikipedia (online).
- ³² C. P. Bean and D. S. Rodbell, *Phys. Rev.* **126**, 104 (1962).
- ³³ D. J. Bergmann and B. I. Halperin, *Phys. Rev. B* **13**, 2145 (1976).
- ³⁴ It may be easy to overlook this simple relationship for inversion symmetry: according to Referee C of arXiv:1012.5127. ; "... the inversion about the origin is ... not present in Table I among the other generators." A count of symmetry operations, 4 for \mathcal{R}_4 , 2 for m_d , and 2 for m_z , indicates that Table I does include all 16 operations of the point group, including inversion about the origin.
- ³⁵ Our notation is such that (X', Y', Z') denotes the operation which takes (X, Y, Z) into (X', Y', Z') . Thus $\mathcal{R}_4 = (-Y, X, Z)$.
- ³⁶ See Table 2 of Ref. 19 for a convenient listing of the generators of each space group.
- ³⁷ W. Press, *J. Chem. Phys.* **56**, 2597 (1972).
- ³⁸ E. F. Shender, *Sov. Phys. JETP* **56**, 178 (1982).
- ³⁹ T. Yildirim, A. B. Harris, and E. F. Shender, *Phys. Rev. B* **53**, 6455 (1996).
- ⁴⁰ J. D. Axe, A. H. Moudden, D. Hohlwein, D. E. Cox, K. M. Mohanty, A. R. Moodenbaugh, and Youwen Xu, *Phys. Rev. Lett.* **62**, 2751 (1989). The Landau free energy in this reference is equivalent to what is written here for the case when $\phi_{x,1} = -\phi_{y,2} = Q_1$ and $\phi_{y,1} = -\phi_{x,2} = Q_2$, but without the strain variables.
- ⁴¹ Equivalent structures are those related by rotations and translations. Structures related only by improper rotations (this includes mirrors) may be enantiomorphs and may be from distinct space groups. So here and below we prefer to not invoke improper rotations to test for equivalence.
- ⁴² Note: here and below (except in panel b of Fig. 20 where we make a more convenient choice of axes) we choose the representative to reproduce the setting chosen in Refs. 17 and 19.
- ⁴³ Y. Onodera and Y. Tanabe, *J. Phys. Soc. Jpn* **45**, 1111 (1978).
- ⁴⁴ It is more convenient to replace (\bar{x}, \bar{y}, z) in the set of generators of Ibam given in Ref. 19 by (x, y, \bar{z}) .